Food Engineering Reviews (2021) 13:66–91
https://doi.org/10.1007/s12393-020-09251-y

Authentication and Quality Assessment of Meat Products by Fourier-Transform Infrared (FTIR) Spectroscopy

Kezban Candoğan[1] · Evrim Gunes Altuntas[2] · Naşit İğci[3,4]

Received: 16 March 2020 / Accepted: 14 August 2020 / Published online: 8 September 2020

Abstract

These days, food safety is getting more attention than in the recent past due to consumer awareness, regulations, and industrial competition to offer best quality products. Meat and meat products are very valuable but highly perishable. There is a need for reliable assessment techniques to ensure the safety and quality of these products throughout their shelf life. Classical analytical methods have been replaced with alternative, rapid, simple, and noninvasive methods to enhance productivity and profitability in the meat supply chain. Fourier-transform infrared (FTIR) spectroscopy has become a valuable analytical technique for structural or functional studies related to foods as a rapid, nondestructive, cost-efficient, and sensitive physicochemical fingerprinting method. This technique is readily applicable for routine quality control or industrial applications with a high degree of confidence. FTIR spectroscopy coupled with chemometrics has drawn attention to quality control, safety assessment, and authentication purposes in the meat and meat products domain. This review covers fundamental knowledge on FTIR spectroscopy coupled with chemometric techniques, as well as major applications of this robust method in meat science and technology for adulteration detection, monitoring biochemical and microbiological spoilage and shelf life, determining changes in chemical components such as proteins and lipids.

Keywords Fourier-transform infrared (FTIR) spectroscopy · Chemometrics · Adulteration · Meat quality · Compositional analyses · Safety evaluation

Introduction

Meat is an essential food product for a wholesome diet and is highly appreciated by consumers due to its nutritional value and palatability. The global meat supply is expected to increase over the next decade with an outgrowth of demand contingent on changes in food choice regarding health, nutrition, and diet. An increase of 1.2% in global meat consumption by 2028 compared with the base period (2016–2018) is expected where the demand for valuable meats, like beef, and sheep meats will grow more than others [1]. In order to meet increasing consumer expectations towards manufacturing safe, high quality, sustainable, and cost-effective products, the meat industry and scientists are seeking alternative ways to ensure certain meat quality attributes with extended shelf life and storage stability [2, 3].

Although physical characteristics such as appearance, texture, and color are important quality factors at the time of purchase of meat products; chemical composition and microbiological aspects play a significant role in the eating quality and safety of these products [4, 5, 6]. Authenticity is also an important quality factor for compliance with particular criteria or standard [7, 8]. A number of traditional methods are available for quality and safety evaluation in meat products. Manual controls with experienced inspectors; techniques for evaluating microbial population; significant amount of mechanical, chemical, biochemical, and immunological methods; and sensory analyses are among the classical

✉ Kezban Candoğan
candogan@eng.ankara.edu.tr

Evrim Gunes Altuntas
egunes@ankara.edu.tr

Naşit İğci
igcinasit@yahoo.com.tr

[1] Department of Food Engineering, Faculty of Engineering, Ankara University, Ankara, Turkey

[2] Biotechnology Institute, Ankara University, Ankara, Turkey

[3] Department of Molecular Biology and Genetics, Faculty of Arts and Sciences, Nevşehir Hacı Bektaş Veli University, Nevşehir, Turkey

[4] Science and Technology Application and Research Center, Nevşehir Hacı Bektaş Veli University, Nevşehir, Turkey

approaches to assess meat quality and safety [3, 9]. These traditional methods have some drawbacks such as being time-consuming, destructive, expensive, and involving sophisticated laboratory procedures with tedious sample preparation. Alternative rapid and noninvasive methods are explored for this purpose to enhance productivity and profitability in the meat supply chain [3, 4, 10, 11], to meet consumer demand for superior quality meat products [3, 12].

Vibrational spectroscopy has been one of the most frequently used analytical techniques for assessing quality of meat and meat products for years, as well as for other foods [13–15]. Fourier-transform infrared (FTIR) spectroscopy, which detects molecular vibrations and generates narrow and sharp peaks in the mid-infrared region, has emerged as a nondestructive, rapid, and simple technique for evaluating biological processes due to its ability to carry out multi-analyte assays and to obtain a broad spectrum of information [14, 16–20]. Because it is rapid, simple, and accurate, FTIR spectroscopy, as a physicochemical fingerprinting technique, has been used along with chemometrics in a variety of food products for various purposes. In meat and meat products, FTIR spectroscopy has been used for detection of adulteration (Rodriguez-Saona and Allendorf 2011; [21–25]), monitoring microbiological safety and shelf life [12, 26–29] and also to study the changes in chemical components including proteins and lipids [30–35]. Figure 1 summarizes the applications of FTIR spectroscopy for the analyses in meat and meat products. This review deals with recent research on the possible use of FTIR spectroscopy in detecting and evaluating quality and safety of meat products. Detection of adulteration, spoilage evaluation, and predicting chemical composition are emphasized in particular.

Fundamental Aspects of FTIR Spectroscopy

Infrared spectroscopy is a vibrational spectroscopy technique based on the relationship between the interactions of infrared (IR) radiation with matter. The IR region is divided into three regions, i.e., near infrared (near-IR, 13,500–4000 cm^{-1}, 780–2500 nm), mid-infrared (mid-IR, 4000–400 cm^{-1}; 2500–25,000 nm), and far-infrared (far-IR, 400–10 cm^{-1}; 25,000–1,000,000 nm) [17]. In practice, both near-infrared (NIR) and mid-infrared (MIR) regions are used for the analysis of food, and there are a number of commercial instruments operating in these regions [36, 37]. Fourier-transform, a mathematical process which allows multiplexing the wavelengths in one measurement when used with an interferometer, accelerates the analyses making these approaches quite useful. As mentioned, this transformation has been commonly used in commercially available spectrometers operating in MIR region whereas dispersive spectroscopy has been usually utilized in NIR region [36]. Because of this, the abbreviation FTIR generally refers to FT-MIR in the specialized literature like in this review [38]. It is the case that recently commercial FT-NIR instruments have become available for food analyses. Both methods, NIR and MIR, have advantages and disadvantages but they will not be addressed in this review. The selection of one method or the other would be based on the performance of them in different regions for a specific sample type, so their advantage depends on the sample type and should be assessed case by case [36, 37, 39].

Fourier-transform infrared spectroscopy is a widely used type of vibrational spectroscopy and one of the oldest approaches for the analysis of various molecules. One of the key parts of an FTIR spectrometer is the interferometer, which

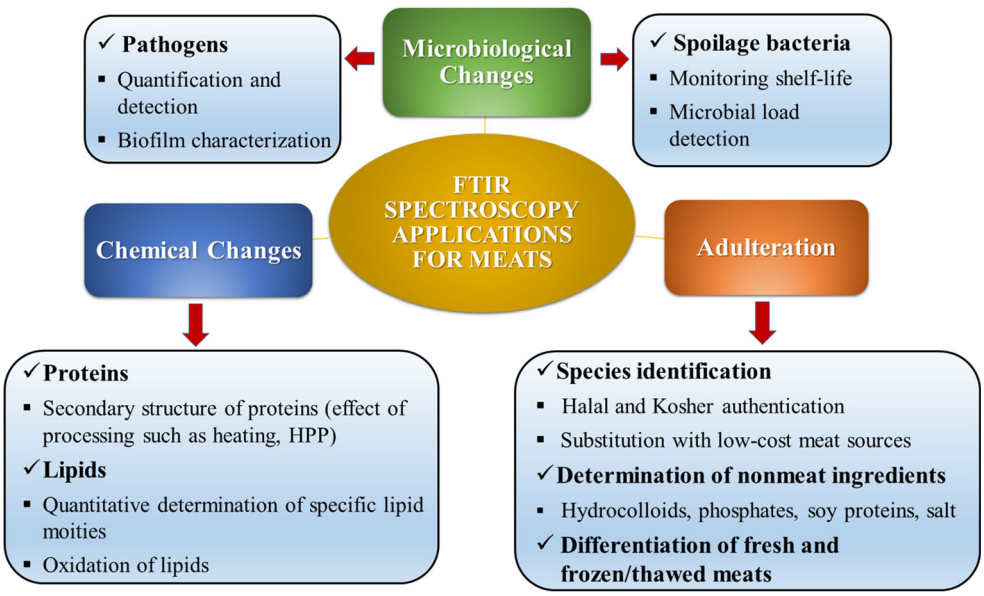

Fig. 1 FTIR spectroscopy applications in meats and meat products

generates an interferogram converted into a typical spectrum by Fourier-transform [16, 37, 40]. In FTIR, IR radiation is absorbed by functional groups in the analyte, which causes vibration of the atoms bonded with covalent bonds. Vibrational excitations that result in a change of the bond dipole produce rising peaks in the IR spectrum. Bond vibrational modes occur in molecules with two or more atoms and can involve changes in bond length (stretching, e.g., symmetrical, asymmetrical) or bond angle (bending, e.g., deformation, rocking, wagging, and twisting) [15, 16, 20, 37, 40–43].

The noninvasive and nondestructive nature of IR radiation makes it a suitable method to analyze biological samples such as tissues, cells, and biological fluids. For this reason, FTIR spectroscopy has become a popular tool in biological analyses in recent years, allowing the extraction of biomolecular information in a rapid and label-free way [16, 19, 44–46]. When IR radiation passes through the sample, each specific vibrational mode absorbs IR at its characteristic frequency, so that each molecule will have its own distinct peak combination resulting in a unique molecular fingerprint of the sample [16, 20, 43, 46–49].

There are three main sampling techniques in FTIR spectroscopy: transmission, transflection (reflection), and attenuated total reflectance (ATR). These methods can be used for both liquid and solid samples [16, 19, 20, 37, 40, 41]. Moreover, gases can also be studied in transmission mode with a special gas cell [50]. In the analysis of meat and meat products, a solid sample prepared from the meat itself or from the extracts of meat such as lipids and proteins is generally needed [8, 21, 24, 51–53]. In transmission spectroscopy, special IR transparent windows separated by a spacer are used for liquids. Solid samples must be in a homogenous powder form (e.g., lyophilized) for transmission. Such samples are generally mixed with IR-transparent matrices such as potassium bromide (KBr) powder. In transflection mode, the analyte is placed on a special IR-reflecting surface (e.g., low-emissivity slides). In ATR, both liquid and solid samples are directly spotted or placed onto the ATR crystal, and pressure is applied to the solid samples with the help of a manifold. A beam of radiation enters the crystal and undergoes total internal reflection. During this process, the analyte absorbs IR at its contact surface with the crystal, resulting in an IR spectrum [16, 19, 20, 37, 40]. One important peculiarity of using ATR is its capability of measuring small dehydrated tissue pieces, which is a useful application for analyzing meat samples, while this is not the case with the KBr pellet method [16, 20, 45].

Adjusting sample thickness prior to the measurement is also one of the important issues in IR spectroscopy, especially in transmission and reflection modes. The sample on the support matrix should be sufficiently thick for obtaining enough intensity and achieving good signal-to-noise ratio. However, too thick samples may result in the nonlinear detector response which might cause problems in quantitative and classification analyses. Also in ATR, the sample loaded on the crystal must have an appropriate thickness providing enough depth of penetration, ideally should be thicker than the penetration depth [16]. Moreover, sample thickness must be standardized to provide the same infrared path length in the sample for avoiding great technical variation and obtaining reproducible spectra [54].

FTIR Spectroscopic Data Analysis in Meat Science

Interpretation and Pre-processing of the FTIR Spectra of Meat Samples

In a typical FTIR absorbance spectrum of any meat sample, the main two parameters are wavenumber (location, frequency) and area/intensity of the peaks. Bandwidth is also useful in providing structural state of the molecules. Based on the relevant literature, it can be determined from which vibration type each peak originates. This information can further be used for assigning peaks to particular chemical groups of the major biomolecules in meat samples such as lipids, proteins, carbohydrates, and nucleic acids [19, 44, 49]. According to the Beer-Lambert law, the area or intensity of an IR absorption peak is proportional to the concentration of associated molecule. Once the peaks are assigned to biomolecules, their alterations can be compared between samples. There is no need to perform absolute quantitation in relative analyses, but it is also possible to determine the amount of a particular compound using one of the appropriate calibration models [19, 20, 40] which are mentioned in the "Statistical Analyses and Chemometrics Applied in FTIR Spectroscopic Analyses of Meat Samples" section.

Before performing statistical tests and chemometric analyses, it is useful to conduct some spectral pre-processing steps [46]. Some of these steps are (1) smoothing, e.g., Savitzky-Golay and wavelet denoising methods ([16, 20, 46, 55]); (2) spectral subtraction [56]; (3) baseline correction, e.g., rubberband method [20, 46]; (4) normalization, e.g., min-max with respect to Amide I band and vector normalization [20, 46]); (5) derivatization [20, 40, 57]; and (6) scatter corrections, e.g., standard normal variate and multiplicative [57]. As pre-processing steps such as baseline correction and normalization alter the resulting peak intensities, caution should be taken and standardization should be ensured when analyzing FTIR spectra [16, 19, 58].

Representative FTIR absorbance spectra of raw beef, pork, and chicken meats in the mid-IR region are shown in Fig. 2; assignments of typical FTIR bands in meat samples are given in Table 1 gathered from Stuart [40]; Naumann [45]; Movasaghi et al. [44]; Rohman et al.

Table 1 Typical FTIR band assignments of meat samples from different species based on relevant literature [20, 21, 23, 40, 44, 45, 51, 52, 59–61]

Wavenumber (cm^{-1})	Definition of the spectral assignment	Related bioorganic molecule in meat sample
3287–3290	Amide A: mainly N–H stretching of proteins, with contribution from O–H stretching of polysaccharides	Proteins, carbohydrates
3068	Amide B: N–H stretching	Proteins
3005–3007	*cis*-olefinic C=H	Lipids
2970	CH_3 asymmetric stretching	Lipids (mainly), proteins
2957–2953	CH_3 asymmetric stretching	Lipids (mainly), proteins
2925–2916	CH_2 asymmetric stretching	Lipids
2875–2870	CH_3 symmetric stretching	Lipids, proteins
2853–2850	CH_2 symmetric stretching	Lipids
1745–1744	C=O carbonyl stretching	Cholesterol esters, triglyceride esters
1715–1711	C=O carbonyl stretching	Fatty acids
1728	Aromatic C=O stretching	Esters
1674	C=C stretching (disubstituted *trans*-olefin)	Lipids
1659	C=C stretching (disubstituted *cis*-olefin)	Lipids
1655–1645	Amide I: 80% C=O stretching, 10% N–H bending, 10% C–N stretching	Proteins (mainly)
1543–1540	Amide II: 60% N–H bending, 40% C–N stretching	Proteins (mainly)
1462–1466	CH_2 bending	Lipids
1456–1455	C–O–H, bending modes of methyl groups	Proteins, lipids
1418–1420	C=H rocking (disubstituted *cis*-olefin)	Lipids
1413–1412	C–N stretching of amides, N–H deformation, C–H deformation	Proteins
1392–1390	COO^- symmetric stretching	Fatty acids
1377–1375	CH_3 bending	Lipids
1340	CH_2 side chain vibrations	Collagen
1314–1205	Amide III: C–N stretching (30%), N–H bending (30%), C=O stretching (10%), O=C–N bending (10%), other (20%)	Proteins
1265	PO_2^- asymmetric stretching (phosphate I)	Nucleic acids, phospholipids
1246–1238	PO_2^- asymmetric stretching (non H-bonded)	Nucleic acids (mainly), phospholipids, phosphorylated proteins
1236–1232	C–O stretching	Esters of lipids
1222–1220	PO_2^- asymmetric stretching	Nucleic acids, phospholipids
1196–1195	C–O stretching	Lipids
1176–1166	CO stretching vibration of C–OH groups of serine, threonine, and tyrosine residues; C–O stretching of carbohydrates	Proteins, carbohydrates
1161–1159	C–O stretching	Esters of lipids
11171113	P–O–C symmetric stretching; C–H bending; C–O stretching	Nucleic acids, fatty acids, esters of lipids
1098–1082	PO_2^- symmetric stretching (fully H-bonded, phosphate 2); C–O stretching; C–H deformation	Nucleic acids, phospholipids, polysaccharides (glycogen), fatty acids, esters of lipids
1060	C–O stretching	Nucleic acids, polysaccharides (glycogen)
1031	C–O stretching	Nucleic acids, lipids
721	CH_2 rocking, C=H bending (*cis* disubstituted olefin)	Lipids

[23]; Severcan et al. [20]; Kurniawati et al. [51]; Igci et al. [61]; Pebriana et al. [52]; Deniz et al. [21]; Fengou et al. [59]; Fengou et al. [60]. As it can be observed in Fig. 2, there are three main regions in the FTIR spectrum. In the first region, between ~ 3600 and 2550 cm^{-1} wavenumbers, bands mostly originating from lipids, and some protein peaks are observable (e.g., C–H, N–H, O–H, CH_2, CH_3 stretching vibrations). The second region between 1700 and 1500 cm^{-1} is the protein region with Amide I and Amide II bands. Amide I band arises from C=O and C–N stretching and N–H bending of proteins while Amide II mainly originates from C–N stretching and N–H bending of peptide bonds (amide groups). The third region between 1450 and 600 cm^{-1} together with protein region is referred to as the fingerprint region which contains many characteristic bands arising from various biomolecules such as

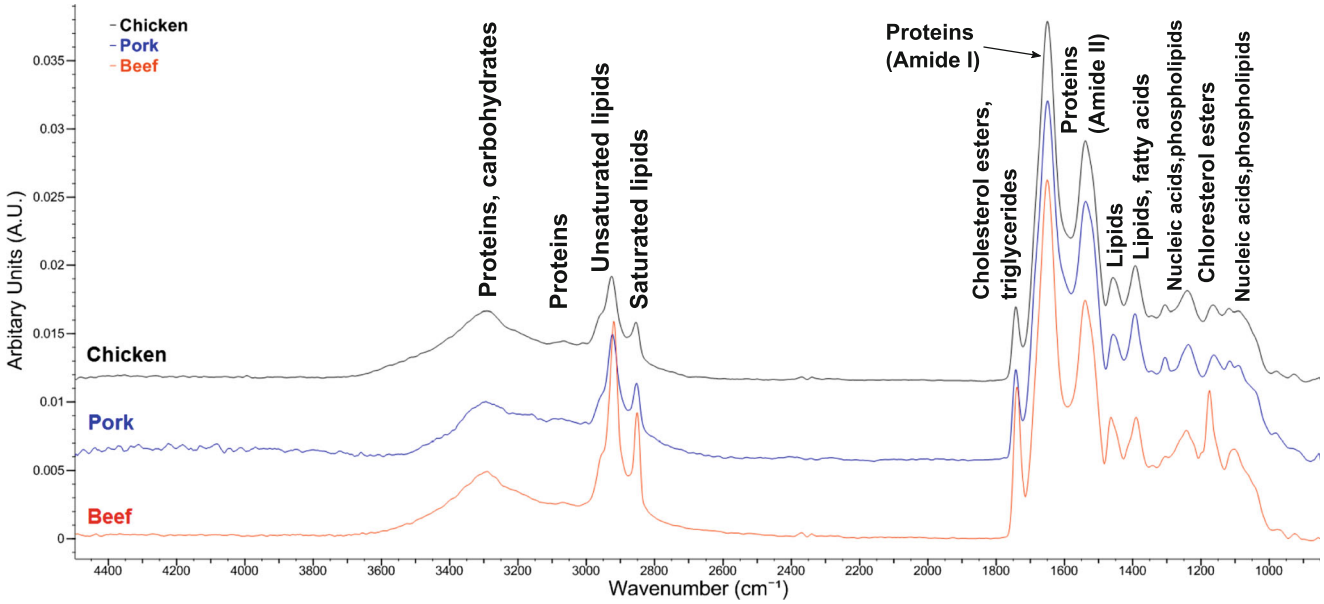

Fig. 2 Representative spectra of chicken, pork, and beef meats (obtained from the *longissimus dorsi* muscle) in the mid-IR region between 4500 and 850 cm^{-1} wavenumbers, showing band assignments for important bioorganic molecules

proteins, lipids, phospholipids, and nucleic acids ([16, 20, 21, 40, 44, 45, 46, 49, 61]).

In addition to peak assignments of the absorbance spectrum, information on the secondary structures of proteins in meat samples can be obtained from the second derivative (and sometimes fourth derivative) spectrum of the Amide I–II region (mainly Amide I band) between 1700 and 1500 cm^{-1} that arise from proteins [20, 40, 56, 62–66]. Absorption maxima appear as minima in the second derivative spectrum. Specific sub-bands in the Amide I region indicate specific secondary structures. Similar to the absorbance spectrum, intensity values of these sub-bands or area values obtained by curve-fitting can be used for relative quantitation [20, 49]. Representative second derivative FTIR spectrum of raw beef in Amide I region is presented in Fig. 3 and corresponding band assignments are given in Table 2.

Statistical Analyses and Chemometrics Applied in FTIR Spectroscopic Analyses of Meat Samples

Although FTIR spectroscopy is a relatively rapid technique regarding sample preparation and measurement time, spectral analyses and chemometrics generally take some time. The most basic statistical analyses that can be used to compare the mean values of two different classes are univariate parametric (e.g., student's *t* test) and non-parametric tests (e.g., Mann-Whitney *U* test). For more than two groups, analysis of variance (ANOVA) in combination with post hoc comparison tests can be used in order to test statistical significance. Calculated band area, intensity, or wavenumber values can be used for these kinds of univariate analyses and they have been used in many published IR spectroscopy-based papers ([20, 46, 68,]).

For the classification and discrimination of the spectra independently from their classes, especially using large data sets or to predict the amount of a compound in complex matrices, multivariate analyses, which are often referred to as chemometrics can be used [15, 16, 19, 20, 46, 69, 70]). This approach has effectively been applied for FTIR spectroscopic analysis and classification of microorganisms [19, 45], plants, gallstones, foods including meat products [15, 21, 42, 69], and pharmaceutical products [71], as well as to discriminate healthy tissues and cells from samples with various diseases such as cancer, diabetes, and other metabolic diseases [19, 45, 61, 67, 72, 73].

Table 2 Characteristic FTIR bands arising from protein secondary structural elements in Amide I region (strong peak between 1700 and 1600 cm^{-1}) based on relevant literature [40, 56, 61, 62, 64, 67]

Wavenumber (cm^{-1})	Assignment (secondary structure)
1610–1620	Aggregated *β*-sheet
1621–1640	*β*-sheet
1641–1647	Random coil/unordered (sometimes overlaps with *a*-helical structure)
1648–1657	*a*-helix
1671–1696	*β*-sheet
1660–1696	Turns and bends, e.g., *β*-turns

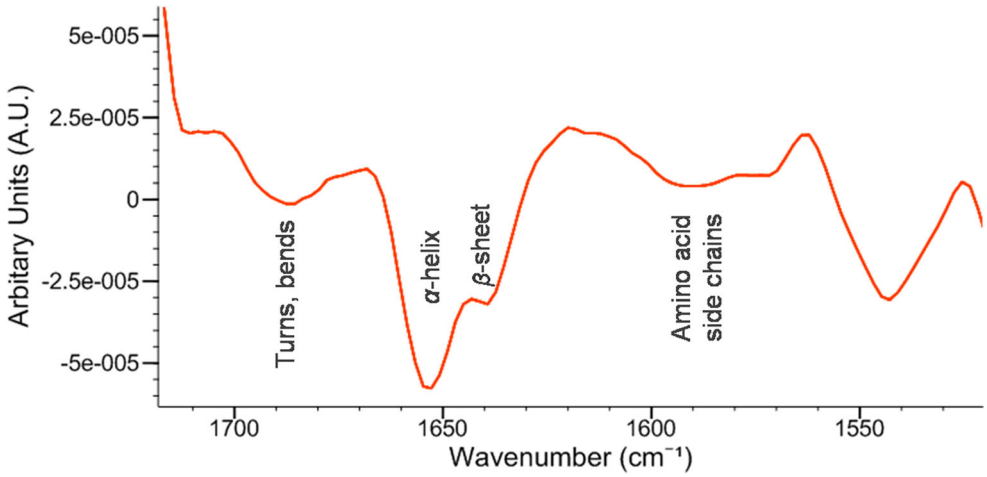

Fig. 3 Representative second derivative spectrum of beef showing sub-bands in the Amide I region (between 1710 and 1580 cm^{-1}). Absorption maxima appear as minima and each sub-band was assigned to particular protein secondary structures based on relevant literature (see Table 2)

Various multivariate analyses with different mathematical models are available and can be divided into two classes: multivariate classification (pattern recognition) and multivariate regression. Multivariate classification can be further divided into unsupervised and supervised techniques [15, 70, 74]. The most frequently used spectral chemometric methods to process FTIR data are listed in Table 3; however, available methods are not limited to those mentioned here [20, 46, 69, 70, 74, 75]). Some of these methods, in particular those used in meat analysis, are briefly described.

In principal component analysis (PCA), one of the unsupervised multivariate classification methods, combinations of variables that vary most between individual samples, is identified by evaluating the total variances within a data set and visualization of the data can be obtained on a *x*-*y* coordinate system. As a powerful data-reduction technique, PCA reduces a large number of initial variables to a smaller data set by choosing the ones with the largest variance. These smaller data sets are called principal components (PCs) and the scatterplot diagrams obtained by PCA are useful for the visualization of the results [16, 20, 70]. This method is widely applied in meat analysis for the classification of meat species, and the detection of spoilage and adulteration (see Tables 4 and 5).

Linear discriminant analysis (LDA) is a frequently used supervised multivariate classification method in FTIR spectroscopic analysis of meat samples with similar purposes as in PCA (see Tables 4 and 5). In LDA, a linear discriminant function of variables (canonical variates) is established based on the differences between the classes in the data set aiming to achieve the maximum separation between classes. LDA considers both within- and between-class variances. LDA can be used in combination with PCA, which is called as PCA-LDA. This analysis is simply an LDA that uses PCs as an input. Partial least squares-discriminant analysis (PLS-DA) is also another discrimination method derived from PLS regression models (PLS is described in more detail below) [20, 69, 70, 74].

Moreover, the use of artificial neural networks (ANNs) has emerged as an alternative supervised pattern recognition chemometric tool since it can be applied to non-linear biospectroscopic data. Being a type of machine learning classifier, ANNs can handle a large amount of data and is especially useful when there is no linear relationship between data sets [20, 46, 70]. This method is useful in both spectroscopy and hyperspectral imaging for classification and can be applied in meat analyses [85, 91]. A comprehensive description of the theory of ANNs is beyond the scope of this review. Briefly, information propagates along interconnected processing units (so-called *neurons*). Each processing unit has its own weighted input and associated non-linear transfer function to be used for transforming input data into an output [70, 77–79]. In a back propagation ANNs approach composed of the three layers (input, hidden, and output), the output signal can be obtained using the following equation;

$$Y_k = f\left(\sum_i W_{ij} X_i - \theta_j\right) \quad (1)$$

where Y_k is the output signal at node k, which is equal to a function of the algebraic sum of the weighted inputs where W_{ij} is the weight between the node i and j, X_i is the input signal at node i, and h is the bias at node j [79]. Once the output signal is produced, the associated error is sent backwards, and weights are adjusted to minimize the aforementioned error. Training (teaching), internal validation, and external validation should be performed to obtain a good model for ANNs [70, 76–79].

Sensitivity, specificity, and precision are important parameters for classification or discrimination models such as cluster analysis (CA), LDA, and PLS-DA to evaluate the performance of the diagnosis. For each region analyzed, these values can be calculated as described below for a hypothetical

Table 3 The most common chemometric tools used in spectral analyses

Method	Features and remarks	References
Unsupervised multivariate classification (pattern recognition) methods		
Hierarchical cluster analysis (HCA)	Does not require an assumption about the number of classes; samples are classified based on similarity and results are demonstrated as dendrograms; different algorithms are available (e.g., Ward s algorithm); qualitative	([70]; [73]; [20]; [16]; [61])
K-means cluster analysis (KMCA)	Requires an assumption about the number of classes; qualitative	([70]; [20]; [16])
Fussy c-means cluster analysis (FCA)	Requires an assumption about the number of classes; qualitative	([70]; [20]; [16])
Principal component analysis (PCA)	A data (dimension) reduction method that reduces the initial number of variables by choosing those with the largest variances (i.e., principal components-PCs); scatterplot diagrams can be plotted; qualitative	([70]; [20]; [75]; [16]; [21])
Supervised multivariate classification (pattern recognition) methods		
Linear discriminant analysis (LDA)	Establishes a linear discriminant function of variables based on differences between classes; qualitative	([70]; [20]; [69]; [74])
Partial least square-discriminant analysis (PLS-DA)	A discriminant analysis that uses PLS models (linear regression); qualitative	([70]; [20]; [69])
PCA-LDA	An LDA that uses PCs as input data; qualitative	([70]; [20]; [69])
Soft independent modelling of class analogy (SIMCA)	A class modelling method that generates PCA models separately for each class in a calibration set and unknown samples are compared with these models; useful for data sets with high within-class variability; qualitative	([70]; [75]; [69]; [74])
Artificial neural networks (ANNs)	A machine learning method that can be applied to both linear and nonlinear data; can handle large amount of data but needs excessive training data; qualitative and quantitative	([76]; [70]; [20]; [77]; [78]; [79])
Support vector machine (SVM)	Requires large data set and low within-class variance like ANN	([80]; [81])
Multivariate regression methods		
Partial least squares regression (PLS-R)	A widely used supervised linear regression method that uses a priori defined classes to build calibration model; applies data reduction to both x and y values; quantitative	([82]; [70]; [69]; [52]; [74])
Principal component regression (PCR)	A supervised method that uses a priori defined classes to build calibration model; applies PCA for data reduction to only x values and PCs are used in training set; quantitative	([70]; [69]; [74])

experiment with one positive/adulterated meat (1) and one control/authentic meat (2) group [73, 97];

$$\text{Sensitivity} = \text{TP}/(\text{TP} + \text{FN}) \quad (2)$$

where TP is the number of samples belonging to group 1 (adulterated) classified in its own cluster (true positive), and FN is the number adulterated samples (group 1) clustered in an authentic group (false negative);

$$\text{Specificity} = \text{TN}/(\text{FP} + \text{TN}) \quad (3)$$

where FP is the number of authentic samples belonging to group 2 clustered in adulterated group (false positive) and TN is the number of authentic samples classified in its own cluster (true negative);

$$\text{Precision} = \text{TP}/(\text{TP} + \text{FP}) \quad (4)$$

Multivariate regression/calibration models are suitable to predict the concentration levels of specific compounds in unknown samples based on the calibration model constructed with a training data set consisting of the spectra of the compound of interest with known concentrations. The information coming from one or more than one peak can be combined in the same model, which makes this approach a suitable and commonly used tool for the detection of adulteration in a meat product (refer to Tables 4 and 5). The most popular

Table 4 Relevant examples of FTIR spectroscopy applications on meat adulteration

Matrix/adulterant/ sample type	Sampling method /analyzed wavenumber range	Pre-processing method	Chemometrics	Remarks	Reference
Beef meatball/pork/-extracted fat	ATR/4000–650 cm^{-1}	No preprocessing	PLS-R	- PLS regression with selected fingerprint regions of 1200–1000 cm^{-1} was an efficient tool in quantifying the level of adulterant pork in meatballs. - R^2 and RMSEC values of 0.999 and 0.128 for actual pork fat value and FTIR predicted values, respectively.	[23]
Ham sausage/pork/direct sausage samples	Transmission (KBr pellet) 4000–400 cm^{-1}	Smoothing, SNV, 1st-order derivative and 2nd derivative	PLS-DA, LS-SVM	- PLSDA with SNV spectra and LS-SVM with second derivative spectra were the best discriminating models with prediction sensitivity of 0.913 and 0.957, and specificity of 0.929 and 0.929, respectively.	[24]
Minced beef/turkey meat/direct meat samples	ATR/4000–700 cm^{-1}	SNV alone or coupled with 1st derivative, Savitzky–Golay derivatization (1st derivative with 11 smoothing points)	PCA, LDA, PLS-R	- Three spectroscopic methods (UV-visible, FT-NIR, and FTIR) were compared with detect turkey meat in minced beef. - FT-NIR and FTIR showed the best performance in prediction with PLS models. - For FTIR data RMSEC ranged from 4.62 to 7.88 and RMSEP from 6.19 to 12.37.	[83]
Fresh and frozen-then thawed beef burger/beef offals (the heart, liver, kidney, and lung)/direct meat samples	ATR/4000–800 cm^{-1}	MSC, SNV transformation and Savitzky–Golay derivatization (1st derivative with 9 smoothing points, 2nd derivative with 11 points)	PCA, PLS-R, PLS-DA, SIMCA	- Spectra from 900–1800 cm^{-1} wavenumber range were used for chemometrics. - PLS provided 100% correct classification accuracies separately for fresh and frozen-then-thawed samples. - High sensitivities (0.94 to 1.0) in separate class-models for fresh and thawed samples, lower specificities (0.33–0.80) for fresh and 0.41–0.87 for thawed burgers. - Sensitivity 1.0, specificity 0.29–0.91 when both sample types were modeled together.	[25]
Beef jerky/pork /powdered samples	ATR/4000–700 cm^{-1}	Baseline correction, normalization by value, smoothing (13-points)	LDA, SIMCA and SVM	- For detection of adulteration, in chemometric analysis, the best model was LDA on the data obtained from the whole spectra with 100% accuracy of classifying and predicting of the sample.	[84]
Beef meatball/rat meat/-extracted fat	ATR/4000–400 cm^{-1}	No preprocessing	PCA, PLS-R	- The 750–1000 cm^{-1} wavenumber range was employed for quantitative analysis. - For quantification using PLS, R^2 and RMSEC values were 0.993 and 1.79%, respectively. - PCA was efficient in the classification of rat meat and beef in meatball formulation.	[22]
Raw chicken meat/frozen-thawed chicken meat/dried "press juice"	HTS-XT microplate adapter/4000–500 cm^{-1}	Second derivatives of the original spectra with a 9-point Savitzky-Golay filter; vector normalization	HCA, ANN	Significant differences at 1660–1628 cm^{-1} (protein region) between raw and frozen-thawed samples related to α-helical (1651 cm^{-1}) and β-plated sheet (1639 cm^{-1}, 1633 cm^{-1}) protein secondary structures.	[85]

Table 4 (continued)

Matrix/adulterant/ sample type	Sampling method /analyzed wavenumber range	Pre-processing method	Chemometrics	Remarks	Reference
				- ANN exhibited more correct classification than HCA for samples subjected to shorter periods of frozen storage.	
Bovine meat/injected non-meat ingredients (NaCl, phosphates, carrageenan, maltodextrin)/direct meat samples	ATR/4000–525 cm^{-1}	Savitzky-Golay smoothing (15 points in filter and second order polynomial fit), MSC and class centroid centering	PCA, the main focus on PLS-DA, low-, and medium level data fusion	- With data fusion model, 91% of the adulterated meats was accurately detected. - Existence of NaCl, tripolyphosphate, and carrageenan was associated to certain infrared bands. - For NaCl addition to bovine meat, the band at about 1690 cm^{-1} with the highest VIP scores due to NaCl effect on specific aggregated β-sheets vibrations of proteins.	[86]
Beef sausage/rat meat/-extracted fat with Bligh and Dyer, Folch, and Soxhlet methods	ATR/4000–450 cm^{-1}	No preprocessing	PLS-R and PCA	- PCA was effective in classifying rat meat and beef lipids extracted using the three methods. - In PLS-R, R^2 and RMSEC for lipid from beef–rat meat sausages extracted by Bligh and Dyer, Folch, and Soxhlet methods were 0.945 and 2.73%; 0.991 and 1.73%; 0.992 and 1.69%, respectively.	[52]
Restructured tilapia/alginate	attenuated transmission and an internal reflection accessory made of composite zinc selenide (ZnSe) and diamond crystals/400–4000 cm^{-1}	Polynomial subtraction and Gaussian smoothing	PLS, PCA	- With both PLS and PCA, it was possible to quantitative analyze different concentrations of sodium alginate. - For quantification, R^2 and RMSEC values were 0.998 and 2.00%, respectively. - For the classification of lower and higher concentrations of sodium alginate, PCA was successful.	[87]
Beef mixtures/chicken, turkey/lyophilized samples	ATR/4000–850 cm^{-1}	2^{nd} derivatization; 2^{nd} derivatization + vector normalization; 1^{st} derivatization; 1^{st} derivatization + vector normalization; vector normalization	PCA, HCA	- Effective differentiation with the following regions: - In HCA, 2980–2800 cm^{-1} and 1140–1020 cm^{-1} for chicken; 1290–1210 cm^{-1} and 2880–2800 cm^{-1} for turkey. - In PCA, whole spectrum, 1500–900 cm^{-1}, 1290–1210 cm^{-1}, and 1480–1425 cm^{-1} for both turkey and chicken; 1760–1710 cm^{-1} particularly for chicken.	[21]
Beef meatballs/pork/-extracted fat	ATR/4000–650 cm^{-1}	No preprocessing	PLS-R, PCA	- In PLS, 1022–833 cm^{-1} wavenumber resulted in a successful quantification of pork in meatball formulation with R^2 and RMSEC values of 0.9984 and 1.09%.	[88]
Beef meatballs/dog meat/extracted fat with Bligh-Dyer, and Folch methods	HATR/4000–500 cm^{-1}	No preprocessing	PLS-R, PCA	- In PCA, 1700–700 cm^{-1} region was successful in identification of dog meat in meatball. - In PLS, using Folch method (R^2 = 0.9906; RMESC = 1.80%) resulted in better prediction model than Bligh-Dyer method (R^2 = 0.9860; RMESC = 2.01%) for dog meat.	[89]
Game meat (wild fallow deer)/goat meat	ATR/4000–500 cm^{-1}	Savitzky–Golay smoothing, SNV	PCA, PLS-DA	- PCA was successful in discriminating the adulteration	[90]

Table 4 (continued)

Matrix/adulterant/ sample type	Sampling method /analyzed wavenumber range	Pre-processing method	Chemometrics	Remarks	Reference
				level of the fallow deer in the wavelength range from 2,000 to 900 cm^{-1}. - PLS-DA model is capable of classifying real samples with 100% accuracy; goodness-of-fit value of $R^2Y = 0.62$, goodness-of-prediction value of $Q^2 = 0.51$, and p value = 0.0027.	
Beef/textured soy protein/dried samples	ATR/4000–400 cm^{-1}	Savitzki-Golay smoothing, SNV, MSC, and Min–Max normalization	PCA, PLS-R, ANN	- Wavenumber range of 1700–1071 cm^{-1} was used for data analysis. - Pure beef and beef with soy protein samples were successfully discriminated with PCA. - ANN exhibited an accurate model for discrimination of beef from soy protein with 100% classification accuracy. - For detection of soy protein in beef mixtures, PLS-R provided good results with high R^2 (0.9761) and low RMSECV (0.78%) values.	[91]
Beef/chicken meat/dried samples	ATR and transmittance/4000–400 cm^{-1}	Savitzki-Golay smoothing, SNV, MSC, and min–max normalization	PCA, PLS-R, ANN	- PCA was successful in classification of the adulterated samples even without spectral preprocessing when transmission mode was used. - With preprocessed ATR-FTIR spectrum, ANN showed better results than PLS-R for predicting presence and percentage of chicken meat in the beef meat mixture with an R^2 of 0.999.	[92]
Beef mixtures/pork, horse, and donkey meats/lyophilized samples	ATR/4000–850 cm^{-1}	2^{nd} derivatization; 2^{nd} derivatization + vector normalization; 1^{st} derivatization; MSC; SNV; normalization by max and range	PCA, HCA	- Effective differentiation for adulterated samples within the following regions: - In HCA; 1480–1425 cm^{-1} for donkey meat; 2980–2880 cm^{-1}, whole spectrum (WS) and fingerprint region (1500–900) for horse meat; 1760–1710 and 1210–1190 cm^{-1} for pork. - In PCA, fingerprint region gave good results in all groups.	[93]

ATR attenuated total reflectance, *HATR* horizontal attenuated total reflectance, R^2 coefficient of determination, *RMSEC* root mean square error of calibration, *RMSECV* root mean square error of cross-validation, *RMSEP* root mean square error of prediction, *LS-SVM* least squares support vector machine, *PLS* partial least squares, *PLSR* partial least squares regression, *PLS-DA* partial least squares discriminant analysis, *PCA* principal component analysis, *LDA* linear discriminant analysis, *MSC* multiplicative scatter correction, *SIMCA* soft independent modelling of class analogy, *VIP* variable importance in the projection, *SVM* support vector machine, *SNV* standard normal variate, *ANN* artificial neuronal network

multivariate regression methods are PLS regression (PLS-R) and principle component regression (PCR). These are supervised methods that use a priori defined classes for each spectrum to obtain a teaching data-set to build models (machine-learning approach). These multivariate regression models are later used to predict the class of an unknown spectrum or concentration of a compound. Separate training, testing, and validation sample groups must be used to build quantitative calibration models and the size of these data sets are optimized case-by-case [16, 20, 42, 52, 70].

Table 5 Relevant examples of FTIR spectroscopy applications on microbiological spoilage or quality of meat and meat products

Product	Sampling method/ analyzed wave-number range	Pre-processing method	Chemometrics	Remarks	Reference
Chicken salami	HATR/4000–600 cm^{-1}	Baseline correction	PLS, GA, GP	- GP was used to derive rules showing that at levels of 10^7 bacteria/g. - For both GAs and GP, the region 1088 to 1096 cm^{-1} was the most significant area of the FTIR spectra for the prediction of spoilage of chicken. - FTIR provided a metabolic snapshot and determination of the microbial loads of food samples in 60 s, directly from the sample surface. - This technique may aid in hazard analysis critical control point process for assessment of the microbiological safety of food.	[26]
Minced beef	ATR/4000–650 cm^{-1}	SNV transformation		- Both FT-IR and Raman calibration models gave satisfying results for TVC, LAB, and *Enterobacteriaceae*. - The GA-GP model was better from other programs in predicting the sensory scores using the FT-IR data, but the GA-ANN model performed better in predicting the sensory scores using the Raman data. - Raman spectroscopy and FT-IR spectroscopy were offered as being reliably and accurate method for assessment of meat spoilage.	[94]
Poultry meat	ATR/4000–375 cm^{-1}	SNV transformation	PCA, PLS-DA, SIMCA	- The most acceptable classification results for SIMCA and PLSDA were achieved between 1800 and 1200 cm^{-1}. This spectral window also demonstrated potential for 100% correct classification of chicken salami samples contaminated with *S. enteritidis* and *P. ludensis* from control using SIMCA. - PLS models had better R values for classification (R = 0.984) than predicting various concentration levels (R = 0.939) of poultry specific bacteria. - 800–1200 cm^{-1} wavenumber range yielded few misclassifications using PLS-DA approach.	[95]
Salmon	ATR/2000–900 cm^{-1}	Smoothing based on the Savitzky-Golay algorithm	PCA, PLS-R	- TVC and psychrotrophs, lactic acid bacteria, molds and yeasts, *Brochothrix thermosphacta*, *Enterobacteriaceae*, *Pseudomonas* spp. could be estimated by PLS from the infrared spectral data. - For TVC, the predicted RMSE value was 0.78 log cfu g^{-1} for an external set of samples. - FTIR is declared as a reliable, accurate, and fast method for real-time freshness evaluation of salmon fillets stored under different temperatures and packaging atmospheres.	[28]
Dear and goat meat	ATR/2000–900 cm^{-1}	Smoothing based on the Savitzky-Golay algorithm	PCA, LDA, PLS-R	- PCA analysis showed that wavenumber from 1656 to 1002 cm^{-1} is related to alterations during storage. - LDA data was applied to sustain SA data. - For fallow deer, the RMSE of prediction values were 0.75, 0.61, 0.81, and 0.73 log cfu g^{-1}, for TVC, psychrotrophs, LAB, and *Enterobacteriaceae*, respectively. - For goat, the corresponding values of RMSE were 0.74, 0.68, 0.78, and 0.79 log cfu g^{-1}.	[90]
Ham slices	ATR/4000–650 cm^{-1}	SNV transformation	PLS-R	- Spectral data based on sensory evaluation, classified samples in three quality classes, fresh, semi-fresh, and spoiled. - Bias and accuracy factors were found acceptable for both microbial groups tested for samples without HPP, while for HPP treated samples, values of these indices ranged from 0.963 to 1.332. - FTIR was declared reliable for rapid assessment of sliced ham shelf life.	[96]

Table 5 (continued)

Product	Sampling method/ analyzed wave-number range	Pre-processing method	Chemometrics	Remarks	Reference
Chicken meat	ATR/3000–800 cm^{-1}	Baseline correction	PCA, PLS-R	- Results of total plate count (3.04–8.20 CFU/cm^2) and *Enterobacteriaceae* counts (2.39–6.33 CFU/cm^2) obtained from traditional methods were compared with FTIR spectral data. - ANOVA was applied on data obtained through microbial analyses and results revealed significant changes ($p < 0:05$) in values of microbial load during the storage. - PLS regression analysis permitted estimates of microbial spoilage from spectra with a fit of $R^2 = 0.66$ for total plate count, $R^2 = 0.52$ for *Enterobacteriaceae* numbers.	[12]
Minced pork patties	HATR, MSI/4000–400 cm^{-1}	Savitzky-Golay smoothing with 9-points, SNV, Image pre-processing	PLS-R	- The region between 1800 and 900 cm^{-1} was used for chemometric analysis. - RMSE, log CFU/g for prediction of the test dataset for FTIR and MSI models was 0.915 and 1.173, respectively, while corresponding values of R^2 were 0.834 and 0.727. All methods coupled with PLSR exhibited good potential (better results for FTIR) for prediction of microbiological quality of minced pork.	[59]
Farmed sea bream (Skin or flesh)	HATR, MSI/4000–400 cm^{-1}	Savitzky-Golay 2nd derivatization with 9 smoothing points, image pre-processing	PLS-R	- The region between 1800 and 900 cm^{-1} was used for chemometric analysis. - PLSR models provided quantitative estimations of microbiological quality of fish based on spectral data, in a temperature-independent manner. - The PLSR model based on FTIR data of fish skin showed good performance with R^2 and RMSE values of 0.727 and 0.717, respectively.	[60]

ANN artificial neuronal network, *ATR* attenuated total reflectance, *CFU* colony forming unit, *GA* genetic algorithm, *GP* genetic programming, *HATR* horizontal attenuated total reflectance, R^2 coefficient of determination, *RMSEC* root mean square error of calibration, *RMSECV* root mean square error of cross-validation, *RMSEP* root mean square error of prediction, *LS-SVM* least squares support vector machine, *PLS* partial least squares, *PLS-DA* partial least squares-discriminant analysis, *PCA* principal component analysis, *LAB* lactic acid bacteria, *LDA* linear discriminant analysis, *MSC* multiplicative scatter correction, *MSI* multispectral imaging, *SIMCA* soft independent modelling of class analogy, *VIP* variable importance in the projection, *SVM* support vector machine, *SNV* standard normal variate, *TVC* total viable count

In PCR, PCA is used for data reduction and PCs are generated using the spectra in the training set. Unknowns are predicted based on score vectors derived from their spectra. Unlike PCR and PCA, PLS applies data reduction not only to x values (e.g., wavenumber, frequency), but also to y data (e.g., absorbance intensities) [20, 70, 74]. PLS regression (PLS-R) is the most frequently used multivariate calibration analysis in spectroscopy-based meat identification that uses the two-block predictive PLS model to estimate the relationship between x and y values [15, 82]. Root mean square error (RMSE) of calibration curve (RMSEC), prediction (RMSEP), and coefficient of determination (R^2) values are important parameters which assess the predictive power of a PLS calibration model. RMSE of the cross-validation (RMSECV) is also calculated frequently. Higher predictive power is represented with higher R^2 and lower RMSEC and RMSEP [42, 52]. For PLS calibration models developed to predict the amount of the adulterated meat species, RMSEC and RMSEP can be calculated using the following equations where Yi and $\hat{Y}i$ are the actual and predicted values of an adulterated meat in main species (external validation sample i), respectively; M and N are the number of data in calibration and validation set, respectively [52, 69];

$$\mathrm{RMSEC} = \sqrt{\frac{\sum_{i=1}^{m}\left(\hat{Y}i - Yi\right)^2}{M-1}} \tag{5}$$

$$\mathrm{RMSEP} = \sqrt{\frac{\sum_{i=1}^{n}\left(\hat{Y}i - Yi\right)^2}{N}} \tag{6}$$

In order to achieve the best results in a FTIR spectroscopic study of meat samples, all the steps from sample preparation to measurement and data analysis should be planned well and appropriate methods should be chosen. Figure 4 demonstrates a summary of FTIR spectroscopy analyses steps applied for evaluation of the quality of meat and meat products.

Applications of FTIR Spectroscopy in Meat and Meat Products

FTIR Spectroscopy for Detecting Adulteration in Meat and Meat Products

One of the most important food quality and safety issues worldwide is food fraud or economically motivated adulteration which has been defined by the FDA as "the fraudulent, intentional substitution, or addition of a substance in a product for the purpose of increasing the apparent value of the product or reducing the cost of its production, i.e., for economic gain" [98]). Some common types of food fraud are unapproved enhancement, dilution, tampering, mislabeling, counterfeiting, substitution, and concealment. These fraudulent practices negatively affect the reputation and fair trade of food businesses and consumer rights, posing a significant problem for individuals with ethical or religious concerns, and jeopardize the authenticity of the products. There are also several issues related to food fraud from the legal point of view [7, 84, 86, 99, 100]. Although food fraud has existed since the beginning of the food trade, it has reemerged throughout the world after some recent scandals and has been becoming a threat along the supply chain. Food fraud is estimated to cause more than $ 40 billion losses per year [101].

The most common fraudulent practices applied in meat products are as follows: intentional substitution of premium-quality meats by different types of low-cost meat species; and substitution of ingredients and additives in formulations for financial gain and for improving the sensory and physical characteristics of the end product [7, 8, 102]. Cavin et al. [102] noted several vulnerabilities in raw meat materials and meat products such as substitution of species origin, substitution of meat tissues, substitution of premium meat with lower quality raw meat materials, enhancement of meat protein level, addition of adulterants to increase weight, and concealment using additives. Assessing meat authenticity focusing on determination of species and undesirable ingredients has become a crucial issue in the meat supply chain for regulators and producers as well as for meat scientists and technologists [103, 104]. A variety of standard analytical methods such as histological tests, electrophoretic separation of proteins, immunological procedure, DNA-based techniques, chromatography, and spectroscopic methods are available for identification and authentication in meat and meat products. However, most of them are characterized by being time-consuming, invasive and expensive, and requiring sophisticated laboratory procedures with tedious sample preparation steps. Therefore, research on vibrational spectroscopic methods is now gaining priority due to rapidness and minimum sample preparation requirements. Among these methods, FTIR spectroscopy in meat authentication has gained importance due to its properties as a fingerprint technique, which can be used for

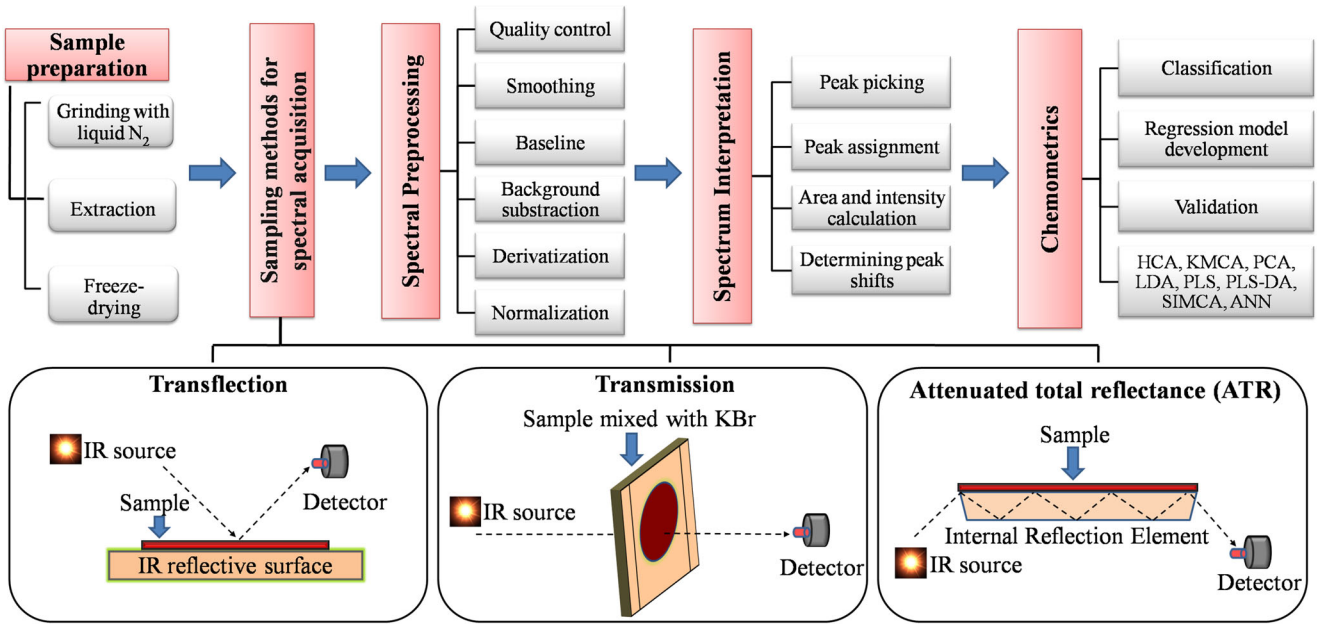

Fig. 4 Schematic diagram of FTIR spectroscopy analyses steps applied for meat and meat products

qualitative and quantitative analyses [7, 8, 15, 21, 23, 35, 53, 86, 88, 89, 92]. Table 4 shows some selected research studies focusing on the detection of meat adulteration by using FTIR spectroscopy.

FTIR Spectroscopy for Identification of Meat Species

Intentional substitution of valuable meats with certain low-cost meat species is a major fraud found in the meat industry. Controlling this type of adulteration is very important for the meat sector and for regulatory agencies in order to protect consumers and verify product authenticity. Several studies using FTIR spectroscopy have been performed for identification and quantification of these fraudulent meat species (Table 4).

Rohman et al. [23] used FTIR spectroscopy and PLS calibration to determine and quantify pork in meatball formulations for halal verification purposes, and noted that it is possible to monitor the adulteration of beef meatballs with pork with FTIR-ATR spectroscopy technique and to quantify the level of pork adulterant successfully at the fingerprint region between 1200 and 1000 cm^{-1}. Xu et al. [24] efficiently discriminated halal and non-halal Chinese ham sausages containing pork using FTIR spectroscopy coupled with chemometric data analysis, i.e., PLS-DA and least squares-support vector machine (LS-SVM).

Rat and dog meats are among the meat types which are not allowed in Muslim and Jewish communities. Rahmania et al. [22] investigated the possibility of using FTIR spectroscopy coupled with PCA and PLS in classification and quantification of rat meat adulterant in beef meatball formulations and reported that FTIR spectroscopy with PLS and PCA data analyses is a robust tool for quantitative analysis of rat meat in beef meatballs at wavenumbers of 1000–750 cm^{-1}. In another study, Rahayu et al. [89] evaluated the feasibility of employing FTIR spectroscopy combined with PLS-R and PCA in qualitative and quantitative analyses of dog meat in beef meatball formulations. Lipid fractions extracted by Foch or Bligh-Dyer method were used for the FTIR analyses. For the product with dog meat and beef, at the wavenumber regions of 1700–700 cm^{-1}, PCA rendered a good classification and PLS-R was a suitable prediction model for quantification. In predicting dog meat adulteration in beef meatball, Folch extraction method yielded a better model with greater R^2, and lower RMSEC and RMSEP values in comparison with Bligh-Dyer method.

One of the most common fraudulent practices in the manufacturing of meat products is to partially substitute the declared ingredients by cheaper ones. Very commonly beef, a premium-quality meat, is substituted with low-priced species such as poultry meat, offal, and mechanically deboned meat. This type of adulteration is a major problem for the traceability in the food supply chain. Alamprese et al. [83] compared FTIR, UV-visible, and NIR spectroscopy combined with chemometrics namely, PCA, LDA, and PLS regression to detect turkey meat adulteration in minced beef. In distinguishing turkey meat from beef, NIR and MIR spectroscopy resulted in the best results. Deniz et al. [21] applied FTIR coupled with hierarchical cluster analysis (HCA) and PCA to detect chicken and turkey meat adulteration. Six characteristic regions were observed for this purpose. Noticeable differences were observed between beef and turkey or chicken meat mixtures based on the distinctive bands from major meat components, particularly related to lipids. A similar study was conducted aiming to detect pork, horse, or donkey meat adulteration in beef-based formulations [93]. Fingerprint region (1500-900 cm^{-1}) and some other spectral regions were found to be useful to differentiate adulterated samples when coupled with PCA and HCA analyses. Mechanically deboned meat is a low-cost and poor quality co-product of the meat industry and may be used as a source of fraudulent substitution [105]. There have been incidences of undeclared utilization of these meats in meat product formulations. Deniz et al. [106] performed a study to detect adulteration of chicken or turkey meat mixtures with mechanically deboned chicken meat (MDCM) by means of FTIR spectroscopy. In secondary structures of proteins, lower relative intensity of α-helix and antiparallel β-sheet structures, and higher relative intensity of β-sheet structures were determined with increasing concentration of MDCM in both chicken and turkey meat mixtures.

FTIR Spectroscopy for Detection of Non-meat Ingredient Substitution

Another common source of adulteration in meat and meat products is addition of non-meat proteins, carbohydrates such as hydrocolloids, cellulose, and starch, or exogenous salts such as phosphates, vegetable fat-based materials which are used to increase water holding capacity and thus, the weight of meat [86, 102]. Concerns about meat authenticity are growing in an exponential fashion due to recent and quite significant fraud scandals. Nunes et al. [86] determined by FTIR-ATR spectroscopy fraud occurred by injecting aqueous solutions of non-meat ingredients (NaCl, phosphates, carrageenan, maltodextrin, collagen) in bovine meat. This study was conducted because of a famous adulteration case in Brazil that developed uproar worldwide because of its consequences in the international meat trade community. Existence of adulterants NaCl, tripolyphosphate, and carrageenan was specifically related to the peaks at 1717–1677 cm^{-1}, 930–890 cm^{-1}, and 1220 cm^{-1}, respectively. The same group of researchers [107] also applied FTIR-ATR spectroscopy to identify frauds in the purge of beef injected with sodium chloride, carrageenan, and tripolyphosphate to increase water retention. The two-class PLS-DA model with around 94–95% reliability rates exhibited the best results when compared with the multi class model

approach in detecting the frauds with the three ingredients. The researchers also applied a soft PLS-DA model together with outlier detection using a set of meat (20 samples) injected with maltodextrin as non-trained adulterant and obtained 100% accurate detection.

Hydrocolloids are generally used in the formulation of processed meat products to increase water retention. In some cases, uncontrolled and intentional addition of these compounds, particularly into the ready-to-eat meats by injection, to make profit results in excessive water content within the product. This type of adulteration, in general, cannot be distinguished by consumers at the time of purchase. Huang et al. [87] investigated the possibility of employing FTIR spectroscopy coupled with PLS and PCA to directly measure sodium alginate used in restructured tilapia fish product at 0, 0.5%, 1.0%, 2.0%, and 5.0% levels. This group developed quantitative and qualitative models for this purpose. PCA based on the wavenumber range between 2000 and 800 cm^{-1} was able to classify lower and higher levels of sodium alginate efficiently. For quantification, R^2 and RMSEC values were 0.998 and 2.00%, respectively, in PLS. Therefore, this method could be applied to differentiate various hydrocolloid incorporations into meat formulations.

Substituting muscle proteins with vegetable proteins such as soy or other bean proteins together with water has also been a common adulteration strategy. Soy proteins are used in the meat industry as meat extenders to increase the water retention, improve texture, and at the same time maintain the total nitrogen content [108]. Excessive amount of addition of these vegetable proteins in the formulations of meat products without declaring in the label is considered a type of adulteration. Keshavarzi et al. [91] investigated the possibility of FTIR-ATR spectroscopy combined with multivariate data analysis for detecting and quantifying textured soy protein in beef mixtures. PCA, ANN, and PLS-R were used for classification and discrimination of the spectra at 1700–1071 cm^{-1} wavenumber range. It was noted that PCA and ANN were successful for accurate differentiation of pure beef from beef containing soy protein. In PLS-R model, a good correlation was obtained with high R^2 value (0.976) and low RMSECV value (0.78%) indicating that FTIR spectroscopy can be used for rapid detection of soy proteins in beef mixtures.

FTIR Spectroscopy for Differentiation of Fresh and Frozen/Thawed Meats

Since quality characteristics of meats are influenced by chemical and physical changes during freezing and thawing, selling meats previously frozen and then thawed without declaring that on the label is considered an economically motivated adulteration. Whether the meat is refrigerated (fresh) or frozen and then thawed prior to sale must be indicated on the label as "defrosted" according to EU Regulation 1169/2011. This situation cannot be perceived at the time of purchasing [85, 109]. Hence, there is a need for rapid and reliable methods to distinguish fresh, and frozen and then thawed meats.

A few studies on discriminating fresh/frozen meat products using FTIR spectroscopy have been conducted. In one of these studies, Zhao et al. [25] investigated the possibility of using FTIR spectroscopy coupled with chemometry (PCA, PLS, PLS-DA, SIMCA-Soft Independent Modelling of Class Analogy) to detect adulteration in fresh and frozen beef burgers by four types of beef offals (the heart, lungs, kidney, and liver). Adulterated samples in fresh and frozen-then-thawed groups were classified using PLS-DA with 100% accuracies. In another study, Alamprese and Casiraghi [110] used FT-NIR and FT-MIR spectroscopy to determine substitution of valuable red mullet and plaice species with low-cost Atlantic mullet and flounder and to evaluate the capability of these methods in discriminating fresh and frozen-thawed fish (Atlantic mullet fillets). FTIR spectroscopy coupled with chemometric tools such as LDA and SIMCA exhibited better results for discrimination of low-cost Atlantic mullet and flounder fillets from those valuable red mullet and plaice fillets, respectively, and also for recognition of fresh and frozen-thawed Atlantic mullet filets. In the prediction attained by using SIMCA, the best results for distinguishing fresh and frozen Atlantic mullet fillets were obtained using the FTIR spectra treated with the multiplicative scatter correction preprocessing. In this analysis, a specificity higher than 95% was determined and sensitivity values were greater than 60% [110].

Grunert et al. [85] employed FTIR spectroscopy to differentiate refrigerated (stored at 4 °C) and frozen/thawed (frozen and stored at − 20 °C for 2, 5, 15, 30, 60, 70, and 85 days) chicken meat in combination with HCA and ANN analyses. HCA was able to differentiate fresh chicken meats from frozen chicken meats for longer periods, while ANN provides identification of frozen samples within even shorter storage periods, i.e., from 2 to 5 days, as well as long storage times for up to 85 days. The results of the aforementioned studies on distinguishing fresh and frozen meat moieties suggest that FTIR spectroscopy in combination with appropriate chemometrics tools could be an alternative rapid and reliable method; however, the performance of the technique needs to be enhanced by employing of improved supervised pattern recognition trained with a larger data set [85, 110].

FTIR Spectroscopy to Assess Chemical Components in Meats

Chemical characteristics of muscle are affected by several ante- and post-mortem factors which determine the ultimate quality of meat and meat products. The major determinants of muscle food quality are proteins, moisture, and lipids which have significant impact on the development of specific

sensorial, nutritional, and physical characteristics such as pH, color, texture, and flavor. Therefore, assessment of these major meat constituents is essential to render possible effects on ultimate product quality [111–113]. FTIR spectroscopy has been applied mainly in determining the levels and changes in two of the major components of meat based products, i.e., proteins [32, 34] and lipids [30, 31, 33].

FTIR Spectroscopy for the Assessment of Proteins

One of the most prevailing applications of FTIR spectroscopy is to monitor the changes in the structure of proteins, particularly in protein secondary structure for better understanding of proteolysis phenomena and thermal behavior of meat proteins [32]. IR spectroscopy has been successfully used for many years to analyze conformational changes and secondary structures of polypeptides and proteins in various states, different concentrations, and diverse environments to assess protein denaturation and protein-protein interactions. Although up to nine characteristic bands can be obtained from IR spectra of polypeptides, the most conspicuous ones are the Amide I and Amide II bands [40]. The Amide I band (1700 − 1600 cm^{-1}), which is extensively used for quantification of the secondary structure and for determining conformational changes in proteins and peptides, mostly arises from the C=O stretching vibrations. The Amide I band takes minor contribution from C − N stretching and N − H bending of the peptide linkages, while the Amide II band, which originates from in-plane N − H bending and C − N stretching vibrations, exhibits less protein conformational sensitivity, but still is useful especially for monitoring side chains [40, 66, 114, 115].

Larrea-Wachtendorff et al. [32] used FTIR spectroscopy to determine the impact of high hydrostatic pressure (HPP) treatments (450 and 550 MPa for 3 and 4 min) on the conformations of the protein secondary structure of palm ruff muscle proteins in prerigor and postrigor states. In the FTIR spectra of secondary structure of prerigor palm ruff proteins, greater α-helix and lower β-sheet structures were detected in comparison with postrigor proteins. On the other hand, no influence of rigor state was determined in the antiparallel β-sheet structure. The HPP treatment affected conformational changes in the secondary structure of palm ruff proteins due to alterations in hydrophobic interactions, hydrogen bonds, and ionic interactions, which was confirmed by FTIR spectra where intramolecular and intermolecular β-sheet conformations showed increases and α-helix and turn structures decrease due to HPP applications.

Sazonova et al. [116] also determined HPP induced changes in protein structure of vacuum packed pork chop samples with FTIR spectroscopy. HPP treated (at 300, 600 MPa for 1 or 15 min) meat and released juice samples, and raw (control) and cooked meats were analyzed with FTIR high-throughput screening. In FTIR spectra of pork muscle, the peak height intensity values of vector normalized spectra indicated that there were decreases in α-helix structure contents in both Amide bands at 1655 and 1548 cm^{-1} and also in β-sheet conformations at 1682 cm^{-1}. An absorption band at 1394 cm^{-1} corresponding to bending vibrations of CH_3 groups in proteins and lipids was observed in all juice sample spectra. It was noted that this band could be a marker for evaluation of changes in proteins as a result of HPP treatments.

In a study by Han et al. [114], FTIR spectroscopy was applied to determine changes in the proteins' secondary structure during heating of pork meat batters at different phase transition temperatures (20 to 74 °C). With the destruction of myosin rods during heat-induced processing of meat batter, the content of α-helix (at 1311 cm^{-1}) decreased and that of β-sheets (near 1235 cm^{-1}) increased indicating myofibrillar protein aggregation.

Ma et al. [34] studied the influence of adding $NaNO_2$ (90 mg/L) on hydroxyl radical-mediated (1 mmol/L of H_2O_2) oxidative damage of yak meat myoglobin to investigate the alterations in the myoglobin structure. For this purpose, four groups of myoglobin extracts solution were prepared: (1) control without addition of H_2O_2 and $NaNO_2$; (2) only H_2O_2 added group without $NaNO_2$ addition; (3) H_2O_2 and $NaNO_2$ added group; and (4) $NaNO_2$ added group without H_2O_2 addition. FTIR spectroscopy was employed to obtain the peaks for evaluating protein secondary structures. The data were extracted from the 1600–1700 cm^{-1} band of the infrared spectrum, analyzed with Gaussian fitting, and the ratios of α-helix, random coil, β-sheet, and β-turns structures of myoglobin were determined. The H_2O_2 added group exhibited higher α-helix and random coil structures content, and lower β-turns structure than the other three groups, indicating that $NaNO_2$ addition could protect the secondary structure of myoglobin from hydroxyl radical-mediated oxidative damage.

In a study by Zhang et al. [117], the changes in secondary structure of myofibrillar proteins of chicken breast muscles subjected to ultrasound-assisted immersion freezing at 125, 165, 205, and 245 W power levels were evaluated in comparison with immersion freezing (without ultrasound) and air freezing. FTIR spectroscopy in the range of 4000–400 cm^{-1} was employed and secondary structure information was extracted in Amide I region by curve fitting. Regarding the changes in the components of Amide I region, decrease in α-helix and β-turn ratios and increase in the β-sheet and random coil were determined in all frozen groups in comparison with the control. The highest ratios of α-helix and β-turn, thus, less damage to the protein secondary structure, were obtained in the samples with the application of ultrasound-assisted immersion freezing at 165 W because this ultrasonic power range resulted in small and regular ice crystal formation [117]

FTIR Spectroscopy for Assessment of Lipids

Analysis of the distribution of lipids and fatty acid composition in meat and meat products is of great importance in terms

of physical and nutritional quality characteristics because it provides information on the fatty acid content of the diet and is advantageous for assessment of carcass quality and for better understanding of the behavior of fat during further processing and shelf life [33, 118, 119]. The most widely used method for determination of fatty acid composition is gas chromatography (GC) analysis which has some limitations such as being time-consuming, laborious and implies utilization of hazardous reagents [31, 33]. For that reason, the focus has been directed to evaluating feasibility of rapid and easier spectroscopy techniques such as FTIR spectroscopy to characterize lipid profiles of meat and meat products [33].

Hu et al. [31] used FTIR-ATR to rapidly determine fatty acid profiles of fat tissues (direct measurement), and solvent-extracted fat from different tissues, namely, subcutaneous, inter-, and intramuscular fats in Wagyu beef. The results from IR spectra of each fat samples were analyzed and the data were compared with GC measurements. In multivariate analyses, the difference among the fatty acid compositions was assessed with PCA, and PLS regression with leave-one-out cross-validation. It was found that it is possible to differentiate subcutaneous fat from inter- and intramuscular fats with PCA using the ATR-FTIR data with regard to fatty acid composition, and to determine the contents of monounsaturated fatty acids (MUFAs) and saturated fatty acids (SFAs) of beef fats, particularly for solvent extracted fats from Wagyu beef.

In another study by Lucarini et al. [33], feasibility of FTIR-ATR spectroscopy coupled with PLS models was investigated to obtain quantitative prediction for the determination of SFA, MUFA, polyunsaturated fatty acid (PUFA), and palmitic acid contents in meat and meat products. Appropriate spectral preprocessing methods (nonfiltering, first derivative, second derivative) and specific spectral ranges were employed for SFA, MUFA, PUFA, and palmitic acid quantification. The most efficient SFA and MUFA models were obtained with the first derivative and at the 3022–650 cm^{-1} region yielding calibration coefficients of 0.9834 and 0.9775, respectively. For PUFA, however, the best performance was achieved for the 4000–650 cm^{-1} region using the first derivative yielding calibration coefficient of 0.9817. Palmitic acid selected as a representative of the single fatty acids exhibited good linear regression for the first derivative in the 4000–650 cm^{-1} region. The authors suggested that the variety and sample numbers in PLS models should be increased in order to improve accuracy for more satisfactory prediction results.

FTIR is considered a useful tool not only to study characterization of fats and oils but also to monitor the changes due to oxidation processes [30, 120]. Guillén and Cabo [30] investigated the characterization and oxidative stability of lipids of pork adipose tissue as influenced by smoke flavorings using FTIR spectroscopy. Dry salting was applied to pork adipose tissue for 24 h followed by immersion smoking using two liquid smoke flavorings for 1, 2, or 3 min. The samples were then subjected to oxidative conditions at 70 °C and analyzed with FTIR spectroscopy after 0, 1, 2, and 4 days under oxidative conditions. Salted and smoked samples exhibited identical FTIR spectra to the control before the oxidation process. However, in the course of oxidation, various changes were observed in FTIR spectra of the samples which are summarized as follows. In the region between 3600 and 3100 cm^{-1}, shifting and broadening of the band with the peak near 3471 cm^{-1} are attributed to overlapping of the original band and of new absorptions due to new compounds formed as a result of oxidation processes. When the ratio between the absorbance of the band at 2854 cm^{-1} and between 3600 and 3100 cm^{-1} (A2854/A3600-3100) was around 90–100, the samples are considered non-oxidized, while with the initiation of oxidation processes, a sharp decrease in this ratio is observed. Thus, shifting of frequency value of the peak around 3471 cm^{-1} and changes in A2854/A3600-3100 ratio can be used as indicators to estimate the oxidation degree in adipose tissue lipids [30]. Other important band found to monitor oxidation of lipids in the aforementioned study was the band near 3007–3006 cm^{-1}. Occurrence of the shifting in the frequency value of this band, as well as the decrease in its absorbance, indicates a decrease in *cis* double bonds and could be used as a measure of oxidation stability in pork adipose tissue lipids. In the control samples subjected to oxidation, a decrease in the absorbance value and shifting of the frequency of the band at 3007–3006 cm^{-1} towards lower wavenumbers was observed from the first day, which proceeded incrementally until the band totally disappeared. However, these changes were determined in the smoked samples during the later days and the band, instead of disappearing, became a shoulder. These changes meant that the samples were at progressive stages of oxidation. The ratio between the absorbance of the band at 2854 cm^{-1} and the band near 3007–3006 cm^{-1} (A2854/A3006) is another measure of the course of oxidation. In control samples the ratio A2854/A3006 showed a sharp increase while slight increases were observed at the beginning which then became more intense in the smoked samples. Changes in the regions between 1800 and 1000 cm^{-1}, and between 1000 and 600 cm^{-1} in the FTIR spectra were attributed to the generation of secondary oxidation products such as aldehydes and ketones [30].

FTIR Spectroscopy for Estimation of Microbiological Changes

Meats are very prone to spoilage as a result of microbiological and biochemical changes. Growth of microorganisms and activity of enzymes elicit alterations in the chemical and structural components of muscle, which further deteriorate the physical and sensory quality of the products [121–123]. On the other hand, consumption of meat and meat products contaminated by pathogenic bacteria constitutes food safety

issues for human health [124]. All of these adverse changes occur in meats due to microorganisms, bringing major challenges for the meat industry and leading to health problems, regulatory compliance issues, and economic losses [125], which are traditionally monitored by sensory testing, chemical methods, and determining microbial population [122]. Among other techniques, FTIR spectroscopy has drawn increasing attention as a propitious method to perform microbiological analyses for various purposes [19, 45]. In this context, the research on the application of FTIR spectroscopy in quantification and detection of pathogens, biofilm characterization, shelf life monitoring, and microbial load detection is reviewed in the following sections. Table 5 summarizes the studies conducted on detecting microbiological changes using FTIR spectroscopy technique in meat and meat products.

FTIR Spectroscopy for Detection of Bacterial Cells

Bacteria are mainly classified in two groups: Gram positive and Gram negative. Gram positive bacteria are distinguished by their thick and rigid layer of peptidoglycan (PG, 40–80% by weight of the cell wall) compared with Gram negative bacteria (10% by weight of the cell wall). Cell wall structure of bacteria consists of parallel polysaccharide chains of alternating *N*-acetylglucosamine (NAG) and *N*-acetylmuramic acid (NAM) residues joined by $\beta(1 \rightarrow 4)$ glycosidic bonds. Besides these bonds, the cell wall of bacteria has parallel chains linked by penta- or tetra-peptides. The amino acid composition of peptide chains can change depending on bacterial species. In one of the best known Gram negative bacteria, *Escherichia coli*, the tetra-peptide consists of D-alanine, D-glutamic acid, and meso-diaminopimelic acid; on the other hand, in Gram positive *Staphylococcus* spp., it consists of L-alanine, D-glutamine, L-lysine, and D-alanine [126–128]. Apart from this difference, Gram positive cell walls contain teichoic acids and lipoproteins that are covalently bound to the PG. Gram negative bacteria have an outer membrane outside the PG layer which contains phospholipids in the inner layer [129].

Based on the differences in the structure of various microorganisms at molecular level, FTIR spectroscopy is considered a promising method to identify or detect bacteria in food complexes by comparing contaminated and uncontaminated spectra and identifying the species with the aid of a previously created spectral database [126, 128]. In a review by Novais et al. [130] on strain typing of various Gram negative and Gram positive bacterial species based on FTIR spectroscopy, it was noted that a consistent correlation between biochemical fingerprints on FTIR spectra and sugar-based coating structures existed. It was also stated that FTIR could be a very useful tool for microbiological evaluations, particularly in pathogen-host interactions because of its strain differentiation performance.

The spectral regions between 3000–2800 cm^{-1} (fatty acid region) and 1700–1500 cm^{-1} (Amide I and Amide II bands of proteins) in FTIR spectra are the most characteristic parts for discriminating bacterial species [131–133]. On the other hand, regions at wavenumbers between 1500–1200 cm^{-1} (mixed region of fatty acid bending vibrations, proteins, and phosphate-carrying compounds), 1200–900 cm^{-1} (absorption bands of the carbohydrates in microbial cell walls), and 900–700 cm^{-1} (fingerprint region for bacteria identification) can be helpful to understand variations in structure and composition of the bacteria [126]. To date, FTIR spectroscopy has been successfully applied for detection or identification of particular foodborne pathogens such as *Listeria*, *E. coli*, *Salmonella*, *Staphylococcus*, *Yersinia*, and *Bacillus*. This technique is not only used for identification but also to exhibit information about bacterial metabolism, growth phase, and antibiotic resistance [94, 126].

In a study by Grewal et al. [95], classification of chicken salami samples based on the FTIR spectral signatures of *Salmonella enteritidis*, *Pseudomonas ludensis*, *Listeria monocytogenes*, and *E. coli* was performed using chemometrics tools. The PLS models exhibited better (higher) *R* values for the classification of bacterial species ($R = 0.984$) compared with quantitation of the bacteria concentration ($R = 0.939$). Classification of chicken salami samples contaminated with *S. enteritidis* and *P. ludensis* from control in the wavenumber region between 1800 and 1200 cm^{-1} was performed by using SIMCA with 100% accuracy while PLS-DA exhibited some misclassifications in this region [95].

Amamcharla et al. [134] studied *Salmonella* contaminated packed beef by analyzing the spectra of headspace volatiles obtained by FTIR spectroscopy coupled with a gas cell and a headspace sampling system. Principal component analysis and statistical classification methods (linear and quadratic discriminate analysis) indicated that whole spectra (4000–500 cm^{-1}) and 850–500 cm^{-1} wavenumber region could be used to discriminate *Salmonella* contaminated beef from uncontaminated samples [134].

FTIR Spectroscopy for Characterization of Biofilms

Some foodborne pathogens can easily attach to the environment of food manufacturing plants and develop biofilms on various surfaces, which further might lead to bacterial cross-contamination during processing. Biofilms mainly comprise of proteins, saccharides, uronic acids, and humic substances, and each biofilm producer microorganism can secrete exopolysaccharides (EPS) with different characteristics depending on its genetic structure and environmental factors [135–137]. FTIR spectroscopy is among the nondestructive approaches used to examine biofilms in situ without changing biofilm structure [138, 139].

One of the biofilm producing food-borne pathogens, *Salmonella*, can create biofilms on a wide variety of food contact surfaces, and might cause a health risk [138, 140]. ATR-FTIR spectroscopy was used by Wang et al. [138] to identify EPS composition of biofilm produced by meat-borne *Salmonella* isolates under a simulated meat manufacturing medium. Spectra of biofilm were obtained at 3500 to 780 cm^{-1} wavenumber range. It was shown that the bands associated with carbohydrates (1084 and 1056 cm^{-1}) and Amides peaks (1647, 1548, and 1539 cm^{-1}) exhibited great intensity indicating that carbohydrates and proteins are essential components of biofilm structure [138].

Wang et al. [141] investigated biofilm development process of five *Enterobacteriaceae* isolates associated with meat processing plants under short- and long-term growth periods. Structure of the mature biofilms from *Proteus mirabilis*, *Citrobacter freundi*, *Enterobacter cloacae*, *Hafnia alvei*, and *Klebsiella oxytoca* was evaluated by FTIR-ATR method and confocal laser scanning microscopy. FTIR-ATR spectra were obtained in the fingerprint region of 2000 to 780 cm^{-1}. Results of the study indicated that in the FTIR-ATR spectra of biofilm structure, the main peaks were corresponded to amide, polysaccharides, and glycosidic linkage [141].

Another meat spoilage and biofilm producing bacteria, *Pseudomonas fluorescens*, were examined by Wang et al. [123]. In this study, the main structure of biofilm EPS of *P. fluorescens* directly on stainless-steel plates after 5 days of incubation was determined from the FTIR-ATR spectra. The results indicate that more than 4.5 log CFU/cm^2 of *P. fluorescens* were transferred to a stainless-steel surface under short-term (5 h) scenario, and bacteria transfer occurred even after only 10 min exposure. A mature biofilm was discovered after 5 days of incubation under long-term (7 days) scenario. The biofilm was characterized by more than 9.5 log CFU/cm^2 cells, 120 mm thick, and a large amount of extracellular polymeric substances. In the FTIR spectra of EPS, the peaks determined at 1650, 1540, 1230, and 1055 cm^{-1} were assigned to the functional groups of proteins (Amide I, Amide II), phosphorus-containing carbohydrates, polysaccharides, and glycosidic linkage deformation of carbohydrates, respectively. These results indicated that the constituents of biofilm EPS formed by *P. fluorescens* mainly were proteins, phospholipids, polysaccharides, and other carbohydrates [123].

In another study, Orhan-Yanikan et al. [139] employed FTIR spectroscopy to determine the effects of two EPS extraction methods, namely, from agar (solid) and from broth (liquid), on the biofilm structure produced by *Acinetobacter baumannii* and *E. coli* strains which were isolated from the production line of a meat processing plant. Biofilms extracted from liquid growth media exhibited more distinct bands when compared with solid growth conditions. In FTIR spectral analysis, protein regions in the range of 4000–550 cm^{-1} wavenumbers were examined. The Amide bands at around 1634 and 1531 cm^{-1} region had great intensity in all biofilms. The main peaks for comparing the two EPS extraction methods were those at 1397 cm^{-1} corresponding to the protein backbone components and carboxylate groups, and at 1230 cm^{-1} corresponding to the general phosphoryl groups and phosphodiester sites of nucleic acids [139].

FTIR spectroscopy for detection of spoilage bacteria

In meat samples, total viable count (TVC) indicates the counts of viable individual microorganisms which may include bacteria, yeasts, and mold species. Spoilage-related microbiota of meat generally consist of *Pseudomonas*, *Brochothrix*, lactic acid bacteria (LAB), *Staphylococcus*, *Micrococcus*, and *Enterobacteriaceae* [90, 142]. LAB are generally known as fermentative bacteria; however, in vacuum or modified atmosphere packaged meats, these Gram positive bacteria easily become predominant spoilage microorganisms. The psychrotrophic strains of Gram negative *Pseudomonas* genus are important for spoilage in aerobically stored meats. Another group of bacteria is the *Enterobacteriaceae* family, which includes hazardous *Salmonella* and *E. coli* strains. Gram positive *Brochothrix thermosphacta* is one of psychrotrophic microorganisms responsible for spoilage in fresh and cured meats [143, 144].

In the past, cultivable bacterial strains could be identified by traditional methods. In fact, microbiologists have only succeeded in discovering a small fraction of bacterial diversity from the huge microbial world. Therefore, some microbial activities cannot be followed by traditional methods and more realistic data about microflora is needed [12, 145]. Biochemical or serological tests or DNA/RNA based molecular techniques exist to identify or detect bacterial species. In order to overcome problems related to these traditionally applied methods, nondestructive, efficient, time-saving, and low-cost methods have drawn attention for evaluating metabolites generated by growth of microorganisms and microbial enzymes [103, 146, 147]. Due to the molecular vibrations of functional groups present in the proteins, nucleic acids, lipids, sugars, and lipopolysaccharides, FTIR spectroscopy can provide information about molecular composition that varies from species to species and even at strain levels. Therefore, the FTIR spectrum is unique and characteristic for each bacterium [126]. It is possible to discriminate a contaminated food from an uncontaminated food with an infrared spectrum if the bacterial metabolism products are specific [95]. FTIR spectroscopy is a technique that could be used to interpret vibrational modes of organic materials and related organisms, and the FTIR spectrum can be a “biochemical signature” of a sample as an indicator for microbiological quality or spoilage level [148]. The main indicators of spoilage (off-odors, discolorations, and slime formation) are detectable after microbial populations reach 10^7 to 10^8 colony forming unit

(CFU)/cm^2 [144]. Therefore, early detection of meat spoilage with low microbial loads is a critical point and possible with spectroscopic techniques.

Ellis et al. [26] investigated the possibility of using FTIR spectroscopy as a tool to determine microbial spoilage directly on the surface of comminuted chicken breast meats. Chicken meat samples were allowed to spoil at room temperature for 24 h. FTIR spectra were obtained using ATR, and classical microbiological plating methods (the total viable count) were simultaneously performed every hour. Bacterial loads were predicted using FTIR spectra combined with PLS-R analysis and machine learning strategies such as genetic algorithms (GAs) and genetic programming (GP). Amide I, Amide II, and free amino acid bands were the most intense peaks that appeared at 1640 cm^{-1}, 1550 cm^{-1}, and 1240–1088 cm^{-1} wavenumber regions, respectively. It was noted that while Amide II band was negatively correlated with spoilage due to the decrease in protein content upon spoilage, there was a positive correlation between spoilage and the peaks at 1240–1088 cm^{-1} (corresponding to free amino acids). Based on the results of GP and GAs, for the spoilage prediction in chicken meats, the 1096–1088 cm^{-1} was the most significant area to differentiate fresh (< 10^7 bacteria/cm^2) and spoiled (≥ 10^7 bacteria/cm^2) samples indicating that proteolysis is the main biochemical indicator of the onset of chicken meat spoilage. It was possible to precisely quantify bacterial contamination of 2 × 10^6 to 2 × 10^9/cm^2 on chicken meat from the FTIR spectra [26]. Furthermore, a similar study was conducted on microbiologically spoiled or contaminated beef [149]. In this study, analyses were performed using the FTIR method in combination with linear regression and evolutionary computational-based machine learning. It was reported that the prediction of bacterial spoilage in beef was not as accurate as used in chicken meat, likely due to the differences in spoilage process in these two types of meats.

FTIR and Raman spectroscopy were compared for microbiological and sensory analysis in minced beef samples under aerobic and modified atmosphere packaging at 5 °C [94]. The data were evaluated with machine learning and evolutionary computing techniques comprising PLS-R, genetic programming (GP), genetic algorithm (GA), ANNs, support vector machines (SVM), and support vector machines regression (SVR). When compared, data evaluation methods using SVM and PLS exhibited slightly more accurate predictions of microbial counts than GA-GP, GA-ANN, GP. Calibration models for both FTIR and Raman provided better predictions for TVC, LAB, and *Enterobacteriaceae*. It was noted that, in general, FTIR models were slightly better in predicting microbial counts.

Kodogiannis and Alshejari [150] utilized FTIR spectra obtained from the surface of the meat for microbiological population prediction and for classification of beef samples in the respective quality classes such as fresh, semi-fresh, and spoiled. Different from other relevant studies, in this research, the proposed model utilized a prototype defuzzification scheme. The neurofuzzy model classification performance was found to be excellent, with 95.94% and 94.74% accuracy for the two different case studies. Prediction performances of multilayer perceptron (MLP) and PLS schemes were very satisfactory. This study was structured to associate FTIR spectra with such systems, and the adaptive fuzzy logic system (AFLS) model used in this study seems very convincing. However, the limited data could be used for evaluation and there is a need to create larger training datasets. The data obtained from classical models such as the adaptive neuro-fuzzy inference system (ANFIS), MLP, and PLS regression were compared against AFLS model introduced as advanced learning-based modelling schemes. The results from these comparisons demonstrated that AFLS modelling could have a great potential for fast and accurate microbial spoilage determination [150].

Microbial spoilage of chicken meat was investigated by Zajac et al. [29] using time-dependent FTIR and Raman techniques. The changes at the amide bonds I, II, III, and S–S, decarboxylation of protein (reduction in the amount of C=O), and their deamination were evaluated to predict poultry meat spoilage in particular. Chicken breast muscle (*pectoralis major*) samples were stored in air at 22 °C up to 10 days and their FTIR and Raman spectra were measured. A deconvolution of the selected bands into Lorentz components was performed for analysis of the obtained spectra. It was reported that this is a reliable approach to detect bacterial and chemical spoilage in meats depending on the biochemical changes occurring during storage, and that the increase in free amino acid content could be successfully used as an indicator for spoilage [29].

The potential of FTIR equipped with ATR to predict the bacterial load of salmon fillets (*Salmo salar*) stored at different temperatures (3, 8, and 30 °C) was measured under three packaging conditions: air packaging (AP) and two modified atmospheres with lemon juice (MAPL) and without lemon juice (MAP) [28]. In the prediction of microbiological population, PLS regression was applied at frequency regions from 1752 to 1735 cm^{-1}, from 1560 to 1245 cm^{-1}, and from 1160 to 1025 cm^{-1} and calibration models were constructed for TVC, psychrotrophs, LAB, mold and yeast, *Brochothrix thermosphacta*, *Enterobacteriaceae*, *Pseudomonas* spp., and H_2S producers. It was reported that for TVC, the RMSEP and R^2 values were 0.78 and 0.81, respectively, indicating good estimates of bacterial counts from the infrared spectral data.

TVC and LAB counts were also successfully estimated in ham slices packaged with probiotic supplemented edible film and/or treated with high pressure processing (HPP) by using FTIR in conjunction with PLS models [96]. The main aim in this study was to classify the samples as fresh, semi-fresh, or

spoiled depending on TVC and LAB counts. In developing PLS regression models to obtain quantitative estimations of microbial counts accuracy (A*f*), bias factors (B*f*), RMSE were calculated. For TVC and lactic acid bacteria, optimum correlation between observations and predictions was determined with B*f* close to 1 in all samples. A*f* was close to 1 for non-HPP treated samples, while it was not the case for HPP treated samples likely due to different spectral characteristics determined in HPP samples in comparison with control samples, resulting from the effect of HPP on texture or flavor properties of the product [96].

Ur Rahman et al. [12] aimed to compare data obtained using traditional methods in detecting microbial spoilage with FTIR in chicken breast fillets. In traditional microbiological analyses, counts for total plate count (TPC) and *Enterobacteriaceae* were between 3.04–8.20 CFU/cm^2 and 2.39–6.33 CFU/cm^2, respectively. Microbial spoilage could be estimated by PLS regression analysis from spectra with a fit of R^2 = 0:66 for TPC, R^2 = 0.52 for *Enterobacteriaceae* numbers, suggesting that FTIR spectral data are useful to retain information regarding the spoilage of poultry meat.

Fengou et al. [59] conducted a study to screen microbiological quality of minced pork using FTIR, visible (VIS) spectroscopy, and multispectral image (MSI) analyses. For FTIR, VIS spectroscopy, and MSI, RMSE (log CFU/g) values were 0.915, 1.173, and 1.034, and R^2 was 0.834, 0.727, and 0.788, respectively. It was noted that FTIR spectroscopy and the other two techniques used in this study would have considerable potential for the prediction of the microbiological quality of minced pork. In another study, FTIR spectroscopy combined with multivariate data analysis was used to estimate microbiological spoilage of farmed sea bream (skin or flesh) during aerobic storage at 0, 4, and 8 °C in comparison with MSI analysis [60]. Spectral data were obtained at wavenumber range of 3100–900 cm^{-1}. PLS-R model performed using the FTIR data of fish skin was successful in monitoring microbial spoilage of fish with R^2, and RMSE predicted values of 0.727 and 0.717, respectively. In the study, MRI models were not satisfactory in predicting microbiological spoilage.

Pavli et al. [151] researched the potential of FTIR spectroscopy in combination with chemometric analysis for estimation of microbiological changes in Greek dry-fermented sausage produced with the addition of probiotic *Lactobacillus plantarum* L125 during fermentation, ripening, and storage at 4 and 12 °C. The relationship between counts determined with microbial analysis and estimated with FTIR spectroscopy for lactic acid bacteria, mesophilic cocci/streptococci, TVC, and staphylococci was evaluated by developing PLS regression models. It was noted that in general, there were good relationships between microbial counts predicted from FTIR data and those obtained from microbiological analyses.

Final Remarks

This review analyzes the many uses of FTIR spectroscopy in meat and meat products where some of the highlights are as follows:

–Aiming to ensure authenticity, quality, and safety of highly nutritious, preferred, and valuable meat products, scientists, food authorities, and the food industry need to develop alternative, reliable, and rapid assessment techniques to overcome the limitations of traditional methods. Among several qualitative and quantitative methods, FTIR spectroscopy has been employed for various quality and process control purposes in the food industry because it offers excellent opportunities for structural and functional studies.

–In addition to being fast, sensitive, and safe, FTIR spectrometers provide simple and nondestructive measurements without the need of complicated, time-consuming sample preparation. Current research on this technique has focused on identification of origin or species, compositional analyses, and detection of microbiological and chemical changes in meat products

–The eligibility of this robust analytical technique over more classical methods is evident. Nonetheless, it must be noted that FTIR spectroscopy would have a good chance to become successful only if it is coupled with chemometric modelling. Proper selection of statistical data analysis is necessary for an accurate interpretation of collected data.

–One of the main drawbacks in FTIR spectroscopic analysis of meat samples is that there is no standard universal application to achieve a consensus on measurement, spectral pre-processing, and chemometrics methods. Studies on FTIR spectroscopic analyses of tissues focusing on biomedical/diagnostic applications suggest a standardized workflow based on the goals and scope of the experiment [16]. Such approach could be used to develop standard laboratory protocols in the field of meat science and technology to improve the performance of this technique.

–Sample type, i.e., different meat species; different muscles from the same carcass; raw meat, or processed meat, should also be considered when selecting an appropriate chemometric model. Furthermore, because of the possible heterogeneity of the meat samples, proper sample preparation before analysis should be chosen since FTIR spectrometers measure a small portion from the meat samples. Application of more than one chemometric method for each case to process data from a given type of meat sample would improve the performance and make FTIR spectroscopy more precise and reliable, and thus widen its scope of application.

–Although it adds extra steps, extraction of specific food components (e.g., fat, protein) could be considered in some cases for the detection of adulteration if the specificity, sensitivity, and power of the model are significantly increased. Such is the case of processed meats substituted with unwanted

meat species and incorporated with undeclared additives. Therefore, when differentiation is based on spectral data related to specific muscle components, a good compromise between results obtained from the extracted constituent and from direct meat tissue measurement should be reached to warrant the accuracy of the application.

–Validation is an important element for diagnostic analytical techniques, thus, for FTIR spectroscopy as well. After mathematical model validation steps, results should be compared with other standard methods in order to assess its limits, suitability, and accuracy.

–The number of published papers regarding the application of FTIR spectroscopy among other spectroscopic methods in the analysis of meat and meat products has increased rapidly, especially in the past 5 years, and such studies have gained attention because of its many advantages. With the growth of knowledge on the application of vibrational spectroscopy in food science, instruments and software specializing in food analysis will probably appear in the market as an end-user product. Once sufficient knowledge is gained and standardized procedures combined with appropriate chemometric analyses are developed, it will be possible to routinely apply the FTIR spectroscopy method in real practice in meat and other food products.

Acknowledgments The authors gratefully acknowledge financial support from the Scientific and Technological Research Council of Turkey (TÜBİTAK) with Project # 214O182.

Funding This review is funded by the Scientific and Technological Research Council of Turkey (TÜBİTAK), Project # 214O182

Compliance with Ethical Standards

Conflict of interest The authors declare that they have no conflict of interest.

Ethical approval Not applicable

Consent to participate Not applicable

Consent for publication Not applicable

References

1. OECD/FAO (2019) OECD-FAO Agricultural Outlook 2019-2028. OECD Publishing, Paris
2. Grunert KG, Bredahl L, Brunsø K (2004) Consumer perception of meat quality and implications for product development in the meat sector- a review. Meat Sci 66:259–272
3. Troy DJ, Ojha KS, Kerry JP, Tiwari BK (2016) Sustainable and consumer-friendly emerging technologies for application within the meat industry: an overview. Meat Sci 120:2–9
4. ElMasry G, Sun D-W (2010) Meat quality assessment using a hyperspectral imaging system. In: Sun D-W (ed) Hyperspectral Imaging for Food Quality Analysis and Control, 1st edn. Academic Press, New York
5. Herrero AM (2008) Raman spectroscopy a promising technique for quality assessment of meat and fish: a review. Food Chem 107: 1642–1651
6. Taheri-Garavand A, Fatahi S, Omid M, Makino Y (2019) Meat quality evaluation based on computer vision technique: a review. Meat Sci 156:183–195
7. Abbas O, Zadravec M, Baeten V, Mikuš T, Lešić T, Vulić A, Prpić J, Jemeršić L, Pleadin J (2018) Analytical methods used for the authentication of food of animal origin. Food Chem 246: 6–17
8. Al-Jowder O, Kemsley EK, Wilson RH (1997) Mid-infrared spectroscopy and authenticity problems in selected meats: a feasibility study. Food Chem 59(2):195–201
9. Xiong Z, Sun DW, Pu H, Gao W, Dai Q (2017) Applications of emerging imaging techniques for meat quality and safety detection and evaluation: a review. Crit Rev Food Sci Nutr 57(4):755–768
10. Giaretta E, Mordenti A, Palmonari A, Brogna N, Canestrari G, Belloni P, Cavallini D, Mammi L, Cabbri R, Formigoni A (2019) NIRs calibration models for chemical composition and fatty acid families of raw and freeze-dried beef: a comparison. J Food Compos Anal 83:103257
11. Wojnowski W, Majchrzak T, Dymerski T, Gębicki J, Namieśnik J (2017) Electronic noses: powerful tools in meat quality assessment. Meat Sci 131:119–131
12. Ur Rahman U, Sahar A, Pasha I, ur Rahman S, Ishaq A (2018) Assessing the capability of Fourier transform infrared spectroscopy in tandem with chemometric analysis for predicting poultry meat spoilage. PeerJ 6:e5376
13. Gangidi RR, Proctor A (2009) Meat and Meat Products. In: Sun D-W (ed) Infrared spectroscopy for food quality analysis and control, 1st edn. Academic Press, New York, pp 179–214
14. Li-Chan ECY, Ismail AA, Sedman J, van de Voort FD (2002) Vibrational spectroscopy of food and food products. In: Chalmers JM, Griffiths PR (eds) Handbook of Vibrational Spectroscopy: Applications of Vibrational Spectroscopy in Life, Pharmaceutical and Natural Sciences, 1st edn. John Wiley & Sons Ltd., Chichester
15. Rohman A (2019) The employment of Fourier transform infrared spectroscopy coupled with chemometrics techniques for traceability and authentication of meat and meat products. J Adv Vet Anim Res 6(1):9–17
16. Baker MJ, Trevisan J, Bassan P, Bhargava R, Butler HJ, Dorling KM, Fielden PR, Fogarty SW, Fulwood NJ, Heys KA, Hughes C, Lasch P, Martin-Hirsch PL, Obinaju B, Sockalingum GD, Sulé-Suso J, Strong RJ, Walsh MJ, Wood BR, Gardner P, Martin FL (2014) Using Fourier transform IR spectroscopy to analyze biological materials. Nat Protoc 9(8):1771–1791
17. Bureau S, Cozzolino D, Clark CJ (2019) Contributions of Fourier-transform mid infrared (FT-MIR) spectroscopy to the study of fruit and vegetables: a review. Postharvest Biol Technol 148:1–14
18. Kosa G, Shapaval V, Kohler A, Zimmermann B (2017) FTIR spectroscopy as a unified method for simultaneous analysis of intra- and extracellular metabolites in high-throughput screening of microbial bioprocesses. Microb Cell Factories 16:195
19. Naumann D, Fabian H, Lasch P (2009) FTIR spectroscopy of cells, tissues and body fluids. In: Barth A, Haris PI (eds) Biological and Biomedical Infrared Spectroscopy, 1st edn. IOS Press, Amsterdam
20. Severcan F, Akkas SB, Turker S, Yucel R (2012) Methodological approaches from experimental to computational analysis in vibrational spectroscopy and microspectroscopy. In: Severcan F, Haris PI (eds) Vibrational Spectroscopy in Diagnosis and Screening, 1st edn. IOS Press, Amsterdam

21. Deniz E, Güneş Altuntaş E, Ayhan B, İğci N, Özel Demiralp D, Candoğan K (2018) Differentiation of beef mixtures adulterated with chicken or turkey meat using FTIR spectroscopy. J Food Process Preserv 42(10):e13767
22. Rahmania H, Sudjadi, Rohman A (2015) The employment of FTIR spectroscopy in combination with chemometrics for analysis of rat meat in meatball formulation. Meat Sci 100:301–305
23. Rohman A, Erwanto Y, Man YBC (2011) Analysis of pork adulteration in beef meatball using Fourier transform infrared (FTIR) spectroscopy. Meat Sci 88(1):91–95
24. Xu L, Cai CB, Cui HF, Ye ZH, Yu XP (2012) Rapid discrimination of pork in Halal and non-Halal Chinese ham sausages by Fourier transform infrared (FTIR) spectroscopy and chemometrics. Meat Sci 92(4):506–510
25. Zhao M, Downey G, O'Donnell CP (2014) Detection of adulteration in fresh and frozen beefburger products by beef offal using mid-infrared ATR spectroscopy and multivariate data analysis. Meat Sci 96(2):1003–1011
26. Ellis DI, Broadhurst D, Kell DB, Rowland JJ, Goodacre R (2002) Rapid and quantitative detection of the microbial spoilage of meat by Fourier transform infrared spectroscopy and machine learning. Appl Environ Microbiol 68(6):2822–2828
27. Sahar A, Dufour E (2014) Use of Fourier transform-infrared spectroscopy to predict spoilage bacteria on aerobically stored chicken breast fillets. LWT-Food Sci and Technol 56:315–320
28. Saraiva C, Vasconcelos H, Almeida JMMM (2017) A chemometrics approach applied to Fourier transform infrared spectroscopy (FTIR) for monitoring the spoilage of fresh salmon (*Salmo salar*) stored undermodified atmospheres. Int J Food Microbiol 241:331–339
29. Zajac A, Dyminska L, Lorenc J, Hanuza J (2017) Fourier transform infrared and Raman spectroscopy studies of the time-dependent changes in chicken meat as a tool for recording spoilage processes. Food Anal Methods 10:640–648
30. Guillén MD, Cabo N (2004) Study of the effects of smoke flavourings on the oxidative stability of the lipids of pork adipose tissue by means of Fourier transform infrared spectroscopy. Meat Sci 66:647–657
31. Hu X, Toyoda K, Yamanoue M, Ihara I, Nakai K (2010) Evaluation of fatty acid profile of Wagyu beef by ATR-FTIR spectroscopy. Food Bioprocess Technol 3:883–891
32. Larrea-Wachtendorff D, Tabilo-Munizaga G, Moreno-Osorio L, Villalobos-Carvajal R, Pérez-Won M (2015) protein changes caused by high hydrostatic pressure (HHP): a study using differential scanning calorimetry (DSC) and Fourier transform infrared (FTIR) spectroscopy. Food Eng Rev 7:222–230
33. Lucarini M, Durazzo A, Sánchez del Pulgar J, Gabrielli P, Lombardi-Boccia G (2018) Determination of fatty acid content in meat and meat products: the FTIR-ATR approach. Food Chem 267:223–230
34. Ma G, Chen H, Zhang Q, Ma J, Yu Q, Han L, Chen C, Song R (2019) Protective characterization of low dose sodium nitrite on yak meat myoglobin in a hydroxy radical oxidation environment: Fourier Transform Infrared spectroscopy and laser Micro-Raman spectroscopy. LWT-Food Sci and Technol 116:108556
35. Perisic N, Afseth NK, Ofstad R, Narum B, Kohler A (2013) Characterizing salt substitution in beef meat processing by vibrational spectroscopy and sensory analysis. Meat Sci 95:576–585
36. Rodriguez-Sanoa LE, Allendorf ME (2011) Use of FTIR for rapid authentication and detection of adulteration of food. Annu Rev Food Sci Technol 2:467–483
37. Subramanian A, Rodriguez-Saona L (2009) Fourier transform infrared (FTIR) spectroscopy. In: Sun D-W (ed) Infrared spectroscopy for food quality analysis and control, 1st edn. Academic Press, New York, pp 145–178
38. Griffiths PR (2010) Editorial: FTIR vs. FT-IR vs. mid-IR. Appl Spectrosc 64(2):40A
39. Munjanja BK, Gowera ATD (2017) Dairy products. In: Franca AS, Nollet LML (eds) Spectroscopic methods in food analysis, 1st edn Chapter 21. CRC Press, New York
40. Stuart B (1997) Biological applications of infrared spectroscopy, 1st edn John Wiley & Sons (on behalf of University of Greenwich), Chicester
41. Cozzolino D (2017) Fourier transform spectroscopy. In: Franca AS, Nollet LML (eds) Spectroscopic methods in food analysis, 1st edn. CRC Press, Boca Raton
42. Rohman A, Salamah N (2018) The employment of spectroscopic techniques coupled with chemometrics for authentication analysis of Halal pharmaceuticals. J Appl Pharm Sci 8(10):63–68
43. Sherman Hsu C-P (1997) Infrared spectroscopy. In: Settle FA (ed) Handbook of Instrumental Techniques for Analytical Chemistry, 1st edn. Prentice Hall, New Jersey
44. Movasaghi Z, Rehman S, ur Rehman DI (2008) Fourier transform infrared (FTIR) spectroscopy of biological tissues. Appl Spectrosc Rev 43(2):134–179
45. Naumann D (2001) FT-infrared and FT-Raman spectroscopy in biomedical research. Appl Spectrosc Rev 36(2–3):239–298
46. Trevisan J, Angelov PP, Carmichael PL, Scott AD, Martin FL (2012) Extracting biological information with computational analysis of Fourier-transform infrared (FTIR) biospectroscopy datasets: current practices to future perspectives. Analyst 137(14):3202–3215
47. Baker MJ, Gazi E, Brown MD, Shanks JH, Gardner P, Clarke NW (2008) FTIR-based spectroscopic analysis in the identification of clinically aggressive prostate cancer. Br J Cancer 99(11):1859–1866
48. Boydston-White S, Gopen T, Houser S, Bargonetti J, Diem M (1999) Infrared spectroscopy of human tissue. V. Infrared spectroscopic studies of myeloid leukemia (ML-1) cells at different phases of the cell cycle. Biospectroscopy 5(4):219–227
49. Özel Demiralp FD, İğci N, Peker S, Ayhan B (2014) Temel Proteomik Stratejiler, 1st edn. Ankara Üniversitesi Yayınevi, Ankara
50. Bacsik Z, Mink J, Keresztury G (2004) FTIR spectroscopy of the atmosphere. I. Principles and methods. Appl Spectrosc Rev 39(3):295–363
51. Kurniawati E, Rohman A, Triyana K (2014) Analysis of lard in meatball broth using Fourier transform infrared spectroscopy and chemometrics. Meat Sci 96(1):94–98
52. Pebriana RB, Rohman A, Lukitaningsih E, Sudjadi (2017) Development of FTIR spectroscopy in combination with chemometrics for analysis of rat meat in beef sausage employing three lipid extraction systems. Int J Food Prop 20(S2):S1995–S2005
53. Yang L, Wu T, Liu Y, Zou J, Huang Y, Babu VS, Lin L (2018) Rapid identification of pork adulterated in the beef and mutton by infrared spectroscopy. J Spectrosc 2413874:1–10
54. Blando JD, Porcja RJ, Turpin BJ (2001) Issues in the quantitation of functional groups by FTIR spectroscopic analysis of impactor-collected aerosol samples. Aerosol Sci Technol 35(5):899–908
55. DeNoyer LK, Dodd JG (2002) Smoothing and derivatives in spectroscopy. In: Chalmers JM, Griffiths PR (eds) Handbook of Vibrational Spectroscopy Volume 1: Theory and Instrumentation, 1st edn. John Wiley & Sons, Chicester
56. Adigüzel Y, Haris PI, Severcan F (2012) Screening of proteins in cells and tissues by vibrational spectroscopy. In: Severcan F, Haris PI (eds) Vibrational Spectroscopy in Diagnosis and Screening, 1st edn. IOS Press, Amsterdam
57. Lee L-C, Liong C-Y, Osman K, Jemain AA (2016) Effects of scatter-correction pre-processing methods and spectral derivative

algorithms on forensic classification of paper. AIP Conf Proc 1750(060013):1–9
58. Chalmers JM (2002) Mid-infrared spectroscopy: anomalies, artifacts and common errors. In: Chalmers JM, Griffiths PR (eds) Handbook of Vibrational Spectroscopy: Sample Characterization and Spectral Data Processing, 1st edn. John Wiley & Sons Ltd., Chichester
59. Fengou LC, Spyrelli E, Lianou A, Tsakanikas P, Panagou EZ, Nychas GJE (2019a) Estimation of minced pork microbiological spoilage through Fourier transform infrared and visible spectroscopy and multispectral vision technology. Foods 8(7):238
60. Fengou LC, Lianou A, Tsakanikas P, Gkana EN, Panagou EZ, Nychas GJE (2019b) Evaluation of Fourier transform infrared spectroscopy and multispectral imaging as means of estimating the microbiological spoilage of farmed sea bream. Food Microbiol 79:27–34
61. Igci N, Sharafi P, Demiralp DO, Demiralp CO, Yuce A, Dokmeci S (2017) Application of Fourier transform infrared spectroscopy to biomolecular profiling of cultured fibroblast cells from Gaucher disease patients: a preliminary investigation. Adv Clin Exp Med 26(7):1053–1061
62. Barth A (2007) Infrared spectroscopy of proteins. BBA-Bioenergetics 1767:1073–1101
63. Costantino HR, Chen B, Griebenow K, Hsu CC, Shire SJ (1998) Fourier-transform infrared spectroscopic investigation of the secondary structure of aqueous and dried recombinant human deoxyribonuclease I. Pharm Pharmacol Commun 4(8):391–395
64. Haris PI, Severcan F (1999) FTIR spectroscopic characterization of protein structure in aqueous and non-aqueous media. J Mol Catal B-Enzym 7(1–4):207–221
65. Nabedryk E, Garavito RM, Breton J (1988) The orientation of beta-sheets in porin. A polarized Fourier transform infrared spectroscopic investigation. Biophys J 53(5):671–676
66. Usoltsev D, Sitnikova V, Kajava A, Uspenskaya M (2019) Systematic FTIR Spectroscopy study of the secondary structure changes in human serum albumin under various denaturation conditions. Biomolecules 9(8):359
67. Bozdag G, Igci N, Calis P, Ayhan B, Ozel Demiralp D, Mumusoglu S, Yarali H (2019) Examination of cervical swabs of patients with endometriosis using Fourier transform infrared spectroscopy. Arch Gynecol Obstet 299(5):1501–1508
68. Haaland DM, Jones HDT, Thomas EV (1997) Multivariate classification of the infrared spectra of cell and tissue samples. Appl Spectrosc 51(3):340–345
69. Sikorska E, Khmelinskii I, Sikorski M (2014) Vibrational and electronic spectroscopy and chemometrics in analysis of edible oils. In: Cruz RMS, Khmelinskii I, Vieira M (eds) Methods in Food Analysis, 1st edn. CRC Press, New York
70. Wang L, Mizaikoff B (2008) Application of multivariate data-analysis techniques to biomedical diagnostics based on mid-infrared spectroscopy. Anal Bioanal Chem 391:1641–1654
71. Custers D, Cauwenbergh T, Bothy JL, Courselle P, De Beer JO, Apers S, Deconinck E (2015) ATR-FTIR spectroscopy and chemometrics: an interesting tool to discriminate and characterize counterfeit medicines. J Pharm Biomed Anal 112:181–189
72. Krafft C, Popp J (2012) Diagnosis and screening of cancer tissues by vibrational spectroscopy. In: Severcan F, Haris PI (eds) Vibrational Spectroscopy in Diagnosis and Screening, 1st edn. IOS Press, Amsterdam
73. Severcan F, Bozkurt O, Gurbanov R, Gorgulu G (2010) FT-IR spectroscopy in diagnosis of diabetes in rat animal model. J Biophotonics 3(8–9):621–631
74. Biancolillo A, Marini F (2018) Chemometric Methods for spectroscopy-based pharmaceutical analysis. Front Chem 6:576
75. Stumpe B, Engel T, Steinweg B, Marschner B (2012) Application of PCA and SIMCA statistical analysis of FT-IR spectra for the classification and identification of different slag types with environmental origin. Environ Sci Technol 46(7):3964–3972
76. Udelhoven T, Naumann D, Schmitt J (2000) Development of a hierarchical classification system with artificial neural networks and FT-IR spectra for the identification of bacteria. Appl Spectrosc 54(10):1471–1479
77. Li Z, Zhang X, Mohua GA, Karanassios V (2017) Artificial neural networks (ANNs) for spectral interference correction using a large-size spectrometer and ANN-based deep learning for a miniature one. In: El-Shahat A (ed) Advanced Applications for Artificial Neural Networks, 1st edn. IntechOpen, London
78. Lasch P, Stämmler M, Zhang M, Baranska M, Bosch A, Majzner K (2018) FT-IR hyperspectral imaging and artificial neural network analysis for rapid identification of pathogenic bacteria. Anal Chem 90(15):8896–8904
79. Tao Y, Hsu K, Ihler A, Gao X, Sorooshian S (2018) A two-stage deep neural network framework for precipitation estimation from bispectral satellite information. J Hydrometeorol 19:393–408
80. Bassbasi M, Platikanov S, Tauler R, Oussama A (2014) FTIR-ATR determination of solid non fat (SNF) in raw milk using PLS and SVM chemometric methods. Food Chem 146:250–254
81. Bona M, Marquetti I, Link JV, Makimori GYF, da Costa AV, Lemes ALG, Ferreira JMG, dos Santos Scholz MB, Valderrama P, Poppi RJ (2017) Support vector machines in tandem with infrared spectroscopy for geographical classification of green arabica coffee. LWT-Food Sci Technol 76(B):330–336
82. Wold S, Sjöström M, Eriksson L (2001) PLS-regression: a basic tool of chemometrics. Chemom Intell Lab Syst 58:109–130
83. Alamprese C, Casale M, Sinelli N, Lanteri S, Casiraghi E (2013) Detection of minced beef adulteration with turkey meat by UV–vis, NIR and MIR spectroscopy. LWT-Food Sci Technol 53(1):225–232
84. Kuswandi B, Putri FK, Gani AA, Ahmad M (2015) Application of class-modelling techniques to infrared spectra for analysis of pork adulteration in beef jerkys. J Food Sci Technol 52(12):7655–7668
85. Grunert T, Stephan R, Ehling-Schulz M, Johler S (2016) Fourier transform infrared spectroscopy enables rapid differentiation of fresh and frozen/thawed chicken. Food Control 60:361–364
86. Nunes KM, Andrade MVO, Santos Filho AMP, Lasmar MC, Sena MM (2016) Detection and characterisation of frauds in bovine meat in natura by non-meat ingredient additions using data fusion of chemical parameters and ATR-FTIR spectroscopy. Food Chem 205:14–22
87. Huang H, Grün IU, Ellersieck M, Clarke AD (2017) Measurement of total sodium alginate in restructured fish products using Fourier transform infrared spectroscopy. EC Nutrition 11(1):33–45
88. Guntarti A, Ahda M, Kusbandari A, Sauri AS (2018) Fourier-transform infrared spectroscopy combined with chemometrics for detection of pork in beef meatball formulation. Int J Green Pharm 12(3):153–157
89. Rahayu WS, Martono S, Sudjadi S, Rohman A (2018) The potential use of infrared spectroscopy and multivariate analysis for differentiation of beef meatball from dog meat for Halal authentication analysis. J Adv Vet Anim Res 5(3):307–314
90. Moreira MJP, Silva AC, Almeida JMMM, Saraiva C (2018) Characterization of deterioration of fallow deer and goat meat using microbial and mid infrared spectroscopy in tandem with chemometrics. Food Packag Shelf Life 15:169–180
91. Keshavarzi Z, Banadkoki SB, Faizi M, Zolghadri Y, Shirazi FH (2019) Identification and quantification of texture soy protein in a mixture with beef meat using ATR-FTIR spectroscopy in combination with chemometric methods. Iran J Pharm Res 18(Special Issue):190–197
92. Keshavarzi Z, Banadkoki SB, Faizi M, Zolghadri Y, Shirazi FH (2020) Comparison of transmission FTIR and ATR spectra for discrimination between beef and chicken meat and quantification

of chicken in beef meat mixture using ATR-FTIR combined with chemometrics. J Food Sci Technol 57(4):1430–1438
93. Deniz E, Güneş Altuntaş E, İğci N, Ayhan B, Özel Demiralp D, Candoğan K (2020) Detection of pork, horse or donkey meat adulteration in beef-based formulations by Fourier transform infrared spectroscopy. Gıda 45(2):369–379
94. Argyri AA, Jarvis RM, Wedge D, Xub Y, Panagou EZ, Goodacre R, Nychas GJE (2013) A comparison of Raman and FT-IR spectroscopy for the prediction of meat spoilage. Food Control 29: 461–470
95. Grewal MK, Jaiswal P, Jha SN (2015) Detection of poultry meat specific bacteria using FTIR spectroscopy and chemometrics. J Food Sci Technol 52(6):3859–3869
96. Pavli F, Argyri AA, Nychas GJE, Tasou C, Chorianopoulos N (2018) Use of Fourier transform infrared spectroscopy for monitoring the shelf life of ham slices packed with probiotic supplemented edible films after treatment with high pressure processing. Food Res Int 106:1061–1068
97. Wang Y-Y, Li J-Q, Liu H-G, Wang Y-Z (2019) Attenuated total reflection-Fourier transform infrared spectroscopy (ATR-FTIR) combined with chemometrics methods for the classification of Lingzhi species. Molecules 24(12):2210
98. Federal Register (2009) Volume 74, Issue 64: 15497-15499, April 6
99. Spink J (2016) Food fraud prevention. The International Union of Food Science and Technology (IUFoST) Scientific Information Bulletin (SIB) November 2016:1–12
100. Spink J, Bedard B, Keogh J, Moyer DC, Scimeca J, Vasan A (2019) International survey of food fraud and related terminology: Preliminary results and discussion. J Food Sci 84(10):2705–2718
101. Böhme K, Calo-Mata P, Barros-Velázquez J, Ortea I (2019) Review of recent DNA-based methods for main food-authentication topics. J Agric Food Chem 67(14):3854–3864
102. Cavin C, Cottenet G, Cooper KM, Zbinden P (2018) Meat vulnerabilities to economic food adulteration require new analytical solutions. CHIMIA Int J Chem (Arau) 72(10):697–703
103. Aina GQ, Erwanto Y, Hossain M, Johan MR, Ali ME, Rohman A (2019) The employment of q-PCR using specific primer targeting on mitochondrial cytochrome-b gene for identification of wild boar meat in meatball samples. J Adv Vet Anim Res 6(3):300–307
104. Barakat H, El-Garhy HAS, Moustafa MMA (2014) Detection of pork adulteration in processed meat by species-specific PCR-QIAxcel procedure based on D-loop and cytb genes. Appl Microbiol Biotechnol 98(23):9805–9816
105. Tomaiuolo M, Chiaravalle AE, Mangiacotti M, Petrella A, Di Taranto A, Iammarino M (2019) Innovative techniques for identifying a mechanically separated meat: sample irradiation coupled to electronic spin resonance. Eur Food Res Technol 245:2331–2341
106. Deniz E, Güneş Altuntaş E, Ayhan B, Özel Demiralp D, Candoğan K (2017) Identification of mechanically deboned meat adulteration by FTIR spectroscopy in chicken and turkey meat formulations in terms of meat components structure. 2nd Congress on Food Structure and Design. 26-28 October, Antalya. Turkey
107. Nunes KM, Andrade MVO, Almeida MR, Sena MM (2020) A soft discriminant model based on mid-infrared spectra of bovine meat purges to detect economic motivated adulteration by the addition of non-meat ingredients. Food Anal Methods 13:1699–1709. https://doi.org/10.1007/s12161-020-01795-3
108. Brewer MS (2012) Reducing the fat content in ground beef without sacrificing quality: a review. Meat Sci 91:385–395
109. Górska-Horczyczak E, Horczyczak M, Guzek D, Wojtasik-Kalinowska I, Wierzbicka A (2017) Chromatographic fingerprints supported by artificial neural network for differentiation of fresh and frozen pork. Food Control 73:237–244
110. Alamprese C, Casiraghi E (2015) Application of FT-NIR and FT-IR spectroscopy to fish fillet authentication. LWT-Food Sci Technol 63(2015):720–725
111. Estévez M (2011) Protein carbonyls in meat systems: a review. Meat Sci 89:259–279
112. Guyon C, Meynier A, de Lamballerie M (2016) Protein and lipid oxidation in meat: a review with emphasis on high pressure treatments. Trends Food Sci Technol 50:131–143
113. Wood JD, Enser M, Fisher AV, Nute GR, Sheard PR, Richardson RI, Hughes SI, Whittington FM (2008) Fat deposition, fatty acid composition and meat quality: a review. Meat Sci 78:343–358
114. Han Z, Zhang J, Zheng J, Li X, Shao JH (2019) The study of protein conformation and hydration characteristics of meat batters at various phase transition temperatures combined with low-field nuclear magnetic resonance and Fourier transform infrared spectroscopy. Food Chem 280:263–269
115. Kong J, Yu S (2007) Fourier transform infrared spectroscopic analysis of protein secondary structures. Acta Biochim Biophys Sin 39:549–559
116. Sazonova S, Grube M, Shvirksts K, Galoburda R, Gramatina I (2019) FTIR spectroscopy studies of high pressure-induced changes in pork macromolecular structure. J Mol Struct 1186: 377–383
117. Zhang C, Li X, Wang H, Xia X, Kong B (2020) Ultrasound-assisted immersion freezing reduces the structure and gel property deterioration of myofibrillar protein from chicken breast. Ultrason Sonochem 67:105–137
118. Ansorena D, Astiasarán I (2008) Ingredients: meat, fat, and salt. In: Nollet LML, Toldra F (eds) Handbook of Processed Meats and Poultry Analysis, 1st edn. CRC Press, New York
119. Flåtten A, Bryhni EA, Kohler A, Egelandsdal B, Isaksson T (2005) Determination of C22:5 and C22:6 marine fatty acids in pork fat with Fourier transform mid-infrared spectroscopy. Meat Sci 69:433–440
120. Guillén MD, Cabo N (2000) Some of the most significant changes in the Fourier transform infrared spectra of edible oils under oxidative conditions. J Sci Food Agric 80:2028–2036
121. Argyri AA, Mallouchos AC, Panagou EZ, Nychas GJE (2015) The dynamics of the HS/SPME–GC/MS as a tool to assess the spoilage of minced beef stored under different packaging and temperature conditions. Int J Food Microbiol 193:51–58
122. Huang L, Zhao J, Chen Q, Zhang Y (2014) Nondestructive measurement of total volatile basic nitrogen (TVB-N) in pork meat by integrating near infrared spectroscopy, computer vision and electronic nose techniques. Food Chem 145:228–236
123. Wang H, Cai L, Li Y, Xu X, Zhou G (2018) Biofilm formation by meat-borne *Pseudomonas fluorescens* on stainless steel and its resistance to disinfectants. Food Control 91:397–403
124. Lianou A, Panagou EZ, Nychas GJE (2017) Meat safety-I foodborne pathogens and other biological issues. In: Toldrá F (ed) Lawrie´s Meat Science, 8th edn. Woodhead Publishing Series in Food Science, Technology and Nutrition, pp 521–552
125. Sofos JN (2014) Meat and meat products. In: Motarjemi, J, Lelieverd, H (eds) Food Safety Management, A Practical Guide for the Food Industry. 1st edn Chapter 6. pp. 119-162. Academic Press
126. Davis R, Mauer LJ (2010) Fourier tansform infrared (FT-IR) spectroscopy: a rapid tool for detection and analysis of foodborne pathogenic bacteria. In: Méndez-Vilas A (ed) Current Research, Technology and Education Topics in Applied Microbiology and Microbial Biotechnology, 1st edn. Formatex Research Center, Badajoz
127. Fisher JF, Mobashery S (2020) Constructing and deconstructing the bacterial cell wall. Protein Sci 29:629–646
128. Mauer LJ, Reuhs BL (2008) Mid-Infrared sensors for the rapid analysis of select microbial food borne pathogens. In: Voeller JG

(ed) Wiley Handbook of Science and Technology for Homeland Security, 1st edn. John Wiley & Sons Ltd., Chichester
129. Caveney NA, Li FKK, Strynadka NCJ (2018) Enzyme structures of the bacterial peptidoglycan andwall teichoic acid biogenesis pathways. Curr Opin Struct Biol 53:45–58
130. Novais A, Freitas AR, Rodrigues C, Peixe L (2019) Fourier transform infrared spectroscopy: unlocking fundamentals and prospects for bacterial strain typing. Eur J Clin Microbiol Infect Dis 38:427–448
131. Campos J, Sousa C, Mourão J, Lopes J, Antunes P, Peixe L (2018) Discrimination of non-typhoid *Salmonella* serogroups and serotypes by Fourier transform infrared spectroscopy: a comprehensive analysis. Int J Food Microbiol 285:34–41
132. Helm D, Labischinski H, Schallehn G, Naumann D (1991) Classification and identification of bacteria by Fourier-transform infrared spectroscopy. J Gen Microbiol 137:69–79
133. Sousa C, Novais Â, Magalhães A, Lopes J, Peixe L (2013) Diverse high-risk B2 and D *Escherichia coli* clones depicted by Fourier transform infrared spectroscopy. Sci Rep 3:3278
134. Amamcharla JK, Panigrahi S, Logue CM, Marchello M, Sherwood JS (2010) Fourier transform infrared spectroscopy (FTIR) as a tool for discriminating *Salmonella typhimurium* contaminated beef. Sens & Instrumen Food Qual 4:1–12
135. Bang J, Hong A, Kim H, Beuchat LR, Rhee MS, Kim Y, Ryu JH (2014) Inactivation of Escherichia coli O157: H7 in biofilm on food-contact surfaces by sequential treatments of aqueous chlorine dioxide and drying. Int J Microbiol 191:129–134
136. Díez-García M, Capita R, Alonso-Calleja C (2012) Influence of serotype on the growth kinetics and the ability to form biofilms of Salmonella isolates from poultry. Food Microbiol 31:173–180
137. Srey S, Jahid IK, Ha SD (2013) Biofilm formation in food industries: a food safety concern. Food Control 31:572–585
138. Wang H, Ding S, Wang G, Xu X, Zhou G (2013) In situ characterization and analysis of *Salmonella* biofilm formation under meat processing environments using a combined microscopic and spectroscopic approach. Int J Food Microbiol 167(3):293–302
139. Orhan-Yanikan E, Gulseren G, Ayhan K (2020) Protein profile of bacterial extracellular polymeric substance by Fourier transform infrared spectroscopy. Microchem J 156. https://doi.org/10.1016/j.microc.2020.104831
140. Ariafar MN, Iğci N, Akçelik M, Akcelik N (2019) Investigation of the effect of different environmental conditions on biofilm structure of *Salmonella enterica* serotype Virchow via FTIR spectroscopy. Arch Microbiol 201:1233–1248
141. Wang H, Qi J, Dong Y, Li Y, Xu X, Zhou G (2017) Characterization of attachment and biofilm formation by meat-borne Enterobacteriaceae strains associated with spoilage. LWT 86:399–407
142. McDonald K, Sun DW (1999) Predictive food microbiology for the meat industry: a review. Int J Food Microbiol 52(1–2):1–27
143. He HJ, Sun DW (2015) Microbial evaluation of raw and processed food products by Visible/Infrared, Raman and Fluorescence spectroscopy. Trends Food Sci Technol 46:199–210
144. Wickramasinghe NN, Ravensdale J, Coorey R, Chandry SP, Dykes GA (2019) The predominance of psychrotrophic pseudomonads on aerobically stored chilled red meat. Compr Rev Food Sci Food Saf 18:1622–1635
145. Hameed S, Xie L, Ying Y (2018) Conventional and emerging detection techniques for pathogenic bacteria in food science: a review. Trends Food Sci Technol 81:61–73
146. Aït-Kaddour A, Loudiyi M, Ferlay A, Gruffat D (2018) Performance of fluorescence spectroscopy for beef meat authentication: effect of excitation mode and discriminant algorithms. Meat Sci 137:58–66
147. Sowoidnich K, Schmidt H, Kronfeldta HD, Schwagelec F (2012) A portable 671 nm Raman sensor system for rapid meat spoilage identification. Vib Spectrosc 62:70–76
148. Kodogiannis VS, Pachidis T, Kontogianni E (2014) An intelligent based decision support system for the detection of meat spoilage. Eng Appl Artif Intell 34:23–36
149. Ellis DI, Broadhurst D, Goodacre R (2004) Rapid and quantitative detection of the microbial spoilage of beef by Fourier transform infrared spectroscopy and machine learning. Anal Chim Acta 514: 193–201
150. Kodogiannis VS, Alshejari A (2014) An adaptive neuro-fuzzy identification model for the detection of meat spoilage. Appl Soft Comput 23:483–497
151. Pavli FG, Argyri AA, Chorianopoulos NG, Nychas GJE, Tassou CC (2020) Effect of *Lactobacillus plantarum* L125 strain with probiotic potential on physicochemical, microbiological and sensorial characteristics of dry fermented sausages. LWT Food Sci Technol 118:108810